Citation: Lains Amaral, J., Solá, A.R., Bento dos Santos, T.M., Chichorro, M., 2022. Detrital zircon similarities and dissimilarities between the Iberian Pyrite Belt, Ossa-Morena Zone and Meguma. Geologica Acta, 20.16, 1-19, I-VIII.
DOI: 10.1344/GeologicaActa2022.20.16

geologica acta

Detrital zircon similarities and dissimilarities between the Iberian Pyrite Belt, Ossa-Morena Zone and Meguma

João Lains Amaral[1,2,3] **Ana Rita Solá[1]** **Telmo M. Bento dos Santos[2,3]** **Martim Chichorro[4]**

[1]Laboratório Nacional de Energia e Geologia (LNEG)
Bairro do Zambujal, Apartado 7586- Alfragide, 2610-999 Amadora, Portugal

[2]Universidade de Lisboa, Faculdade de Ciências, Departamento de Geologia
Ed. C6, Piso 4, Campo Grande, 1749-016 Lisboa, Portugal

[3]Universidade de Lisboa, Faculdade de Ciências, Instituto Dom Luiz
1749-016, Lisboa, Portugal

[4]Geobiotec Research Unit, NOVA School of Science and Technology, Dept. Earth Sciences
2829-516, Campus Caparica, Portugal

ABSTRACT

Despite the so-called exotic nature of the South Portuguese Zone relatively to the other major domains of the Iberian Massif of peri-Gondwanan affinity, Devonian detrital rocks of the oldest strata in the Iberian Pyrite Belt have a remarkable resemblance with the Ossa-Morena Zone's Neoproterozoic-Cambrian rocks and the West Meguma's Cambrian-Ordovician rocks, presenting the so-called "West African signature".Using published U-Pb detrital zircon data, we discuss the similarities and dissimilarities between the Iberian Pyrite Belt, Ossa-Morena Zone and West Meguma Terrane through multidimensional scaling, comparing them with other zones of the Iberian Massif, Saxo-Thuringian Zone, Avalonia-Ganderia, and the North African cratonic regions. Our findings show that multidimensional scaling is not entirely effective in displaying the dissimilarities between the peri-Gondwanan terranes due to the background noise caused by the overwhelming number of Cadomian-Panafrican ages. However, it becomes a powerful tool if these ages are filtered. A dominant Meguma-type provenance (Cambro-Ordovician) for the Middle-Upper Devonian rocks of the Iberian Pyrite Belt is demonstrated, mainly attending to their similar Birimian-Eburnean pattern. The possibility of minor contributions from the lower Cambrian rocks of the Ossa-Morena Zone into the Iberian Pyrite Belt quartzites is unlikely, as the latter lack the 1.9Ga peak that characterises the Ossa-Morena Zone sediments. Additionally, the remarkable similarities between Ossa-Morena Zone's and West Meguma's detrital rocks strongly suggest a similar paleogeographic setting (but diachronic) for both terrains from the Ediacaran to Lower Ordovician times relative to the North African blocks.

KEYWORDS **Cadomian-Panafrican. Peri-Gondwanan Paleogeography. Multidimensional Scaling. Birimian-Eburnean Distribution. Iberian Massif.**

INTRODUCTION

The European Variscan Belt is a major structure formed during the collision of Gondwana and Laurussia landmasses (Fig. 1). In the SW Iberian Massif, the South Portuguese Zone (SPZ) is thought to represent a fragment of the Laurussian continent (Braid *et al.*, 2011; Pérez-Cáceres *et al.*, 2017) that collided in the Devonian-Carboniferous with the Ossa-Morena Zone (OMZ), a Gondwana-related terrane (Braid *et al.*, 2018; Ribeiro *et al.*, 2007). Although the pre-Middle Devonian SPZ basement is not exposed, the SPZ comprises Variscan synorogenic volcano-siliciclastic successions distributed in four domains: the Pulo do Lobo Domain (PLD), the Iberian Pyrite Belt (IPB), the Baixo Alentejo Flysch Group and the SW Portugal Domain (Fig. 2) (Oliveira, 2015; Oliveira *et al.*, 2013).

Braid *et al.* (2011) interpreted the detrital zircon signatures of the Middle-Upper Devonian northernmost rocks of the SPZ, the Alajar Melánge within the PLD, as of Laurentia-related provenance marked by abundant Mesoproterozoic zircons. In contrast, the significant occurrence of Mesoproterozoic ages in the Horta da Torre Formation of the PLD (and in the igneous rocks of the SPZ, see also Lains Amaral *et al.* 2021a) suggest, according to Pérez-Cáceres *et al.* (2017), an Avalonian provenance for the SPZ. Thus, respectively, Laurussian inland and margin provenances for the SPZ have been proposed.

The above mentioned sediments of the northern part of the PLD and possibly the IPB pre-Devonian substrate are exotic relatively to the rest of the SPZ (Pérez-Cáceres *et al.*, 2017; Lains Amaral *et al.*, 2021a). Indeed, the quartzites of the IPB, representing a siliciclastic open platform succession (Oliveira *et al.*, 2019), have a typical "West African signature" with a main Cadomian-Panafrican population and a secondary prominent Birimian-Eburnean curve, remarkably similar to the OMZ and West Meguma detrital zircon distributions (Braid *et al.*, 2011). These authors proposed that the few Mesoproterozoic grains in the oldest known IPB rocks indicate a Meguma provenance, as the Meguma detrital rocks also contain minor Mesoproterozoic grains. However, OMZ also hold Mesoproterozoic grains, vestigial in the Cambrian rocks (Sánchez-García *et al.*, 2019) and significant in the Ordovician rocks (Azor *et al.*, 2021). Thus, the OMZ can also be seen as a potential source for the Middle-Upper Devonian sediments of SPZ.

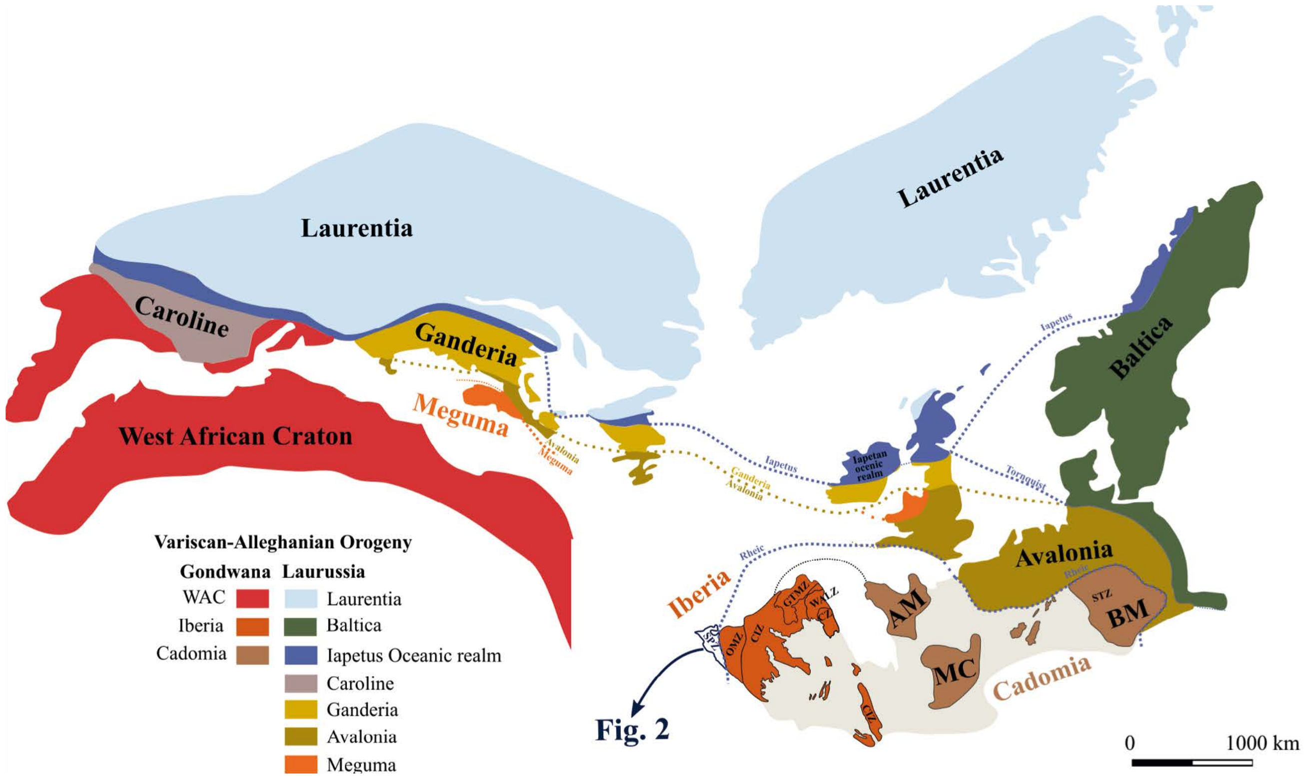

FIGURE 1. Configuration of peri-Gondwanan terranes and main cratonic areas at the end of the Paleozoic (adapted from Couzinié *et al.*, 2019; Henderson *et al.*, 2016). Iberia: Cantabrian Zone (CZ), West Asturian–Leonese Zone (WALZ), Galicia–Trás-os-Montes Zone (GTMZ), Central Iberian Zone (CIZ), Ossa-Morena Zone (OMZ), South Portuguese Zone (SPZ); Cadomia: Amorican Massif (AM), Massif Centrale (MC), Bohemian Massif (BM) which includes Saxo-Thuringia Zone (STZ).

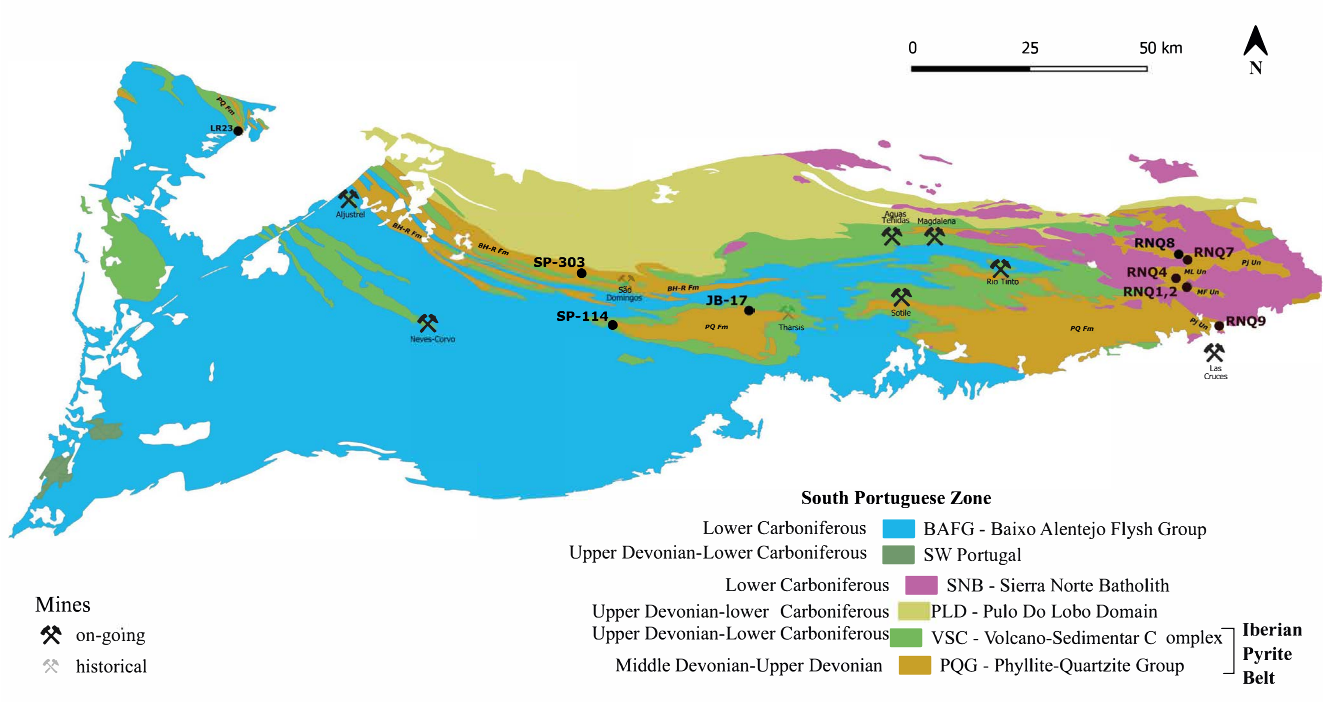

FIGURE 2. Geological map of the South Portuguese Zone adapted from Lains Amaral *et al.* (2021b) and references therein. Black dots: sample locations after Braid *et al.* (2011), Pereira *et al.* (2012b), Pérez-Cáceres *et al.* (2017). PQ Fm: Phyllite–Quartzite Formation; BH-R Fm: Barranco do Homem-Represa Formation; Pj U: Las Pajanosas Unit; LM U: La Minilla Unit; MF U: Media Fanega Unit. In this work, IPB_D is a result of the individual samples: LR23, SP-114, JB-17, RN4, RNQ7, RNQ8, RNQ9.

In this work, using non-metric multidimensional scaling and visual inspection of kernel density estimation and probability density plots of published detrital zircon data, we discuss the provenance of the IPB (included in SPZ) by testing the similarities and dissimilarities with OMZ and West Meguma. Taking into account that the "West African signature" is the most striking feature in these three terranes, the present work will be mostly focused on the Birimian-Eburnean distribution, as this fraction is one of the most important age groups present in West African Craton (WAC), Trans-Sahara belt (TSB) and Saharan Metacraton (SM) (Fig. 3) igneous and metamorphic rocks (Žák *et al.*, 2021), as well as their derived sediments (Cambeses *et al.*, 2017). Consequently, testing the Birimian-Eburnean distribution as a paleogeographic and provenance indicator is also within the scope of the work.

For the sake of comparison, we will include the magmatic-metamorphic zircons from the Gondwanan blocks (WAC, TSB and SM) and detrital zircon data retrieved from Neoproterozoic-Ordovician sediments, other major domains of the Iberian Massif, and other proximal terranes, such as Ganderia and Avalonia. Furthermore, we will include data from the Saxo-Thuringian Zone (STZ), which is often correlated with the OMZ (Rojo-Pérez *et al.*, 2021; Linnemann *et al.*, 2008; Martínez Catalán *et al.*, 2021) and was recently compared to West Meguma (White *et al.*, 2018). The Laurentia-derived Silurian sediments of Ganderia were also included.

Finally, we will discuss the paleogeographic significance, along the North African continent, of such Paleoproterozoic distribution in the Iberian and West Meguma terranes during the Cadomian Orogeny and peripheral Gondwana fragmentation (Fig. 3).

GEOLOGICAL CONTEXT

The Iberian Massif represents the westernmost section of the European Variscan Belt, containing rocks formed during the Cadomian and Variscan cycles (Cambeses *et al.*, 2017; Martínez Catalán *et al.*, 2021; Simancas, 2019). It comprises six major domains (Farias *et al.*, 1987; Julivert *et al.*, 1974; Lotze, 1945), from northeast to southwest: the Cantabrian (CZ), the West Asturian-Leonese (WALZ), the Galicia-Trás-os-Montes (GTMZ), the Central Iberian (CIZ), the Ossa-Morena (OMZ) and the South Portuguese (SPZ) zones (Fig. 1; *e.g.* Simancas, 2019).

It has been widely accepted that the Iberian Massif, except SPZ, is composed of peri-Gondwanan terranes throughout the Paleozoic (Robardet, 2003; Robardet and Gutiérrez-Marco, 2004). The OMZ contains Ediacaran-Carboniferous successions, revealing the development of a Cadomian arc-back-arc system, rifting and drifting related to the opening of the Rheic Ocean and other subsidiary seas, and to the Variscan Orogeny, which led to the

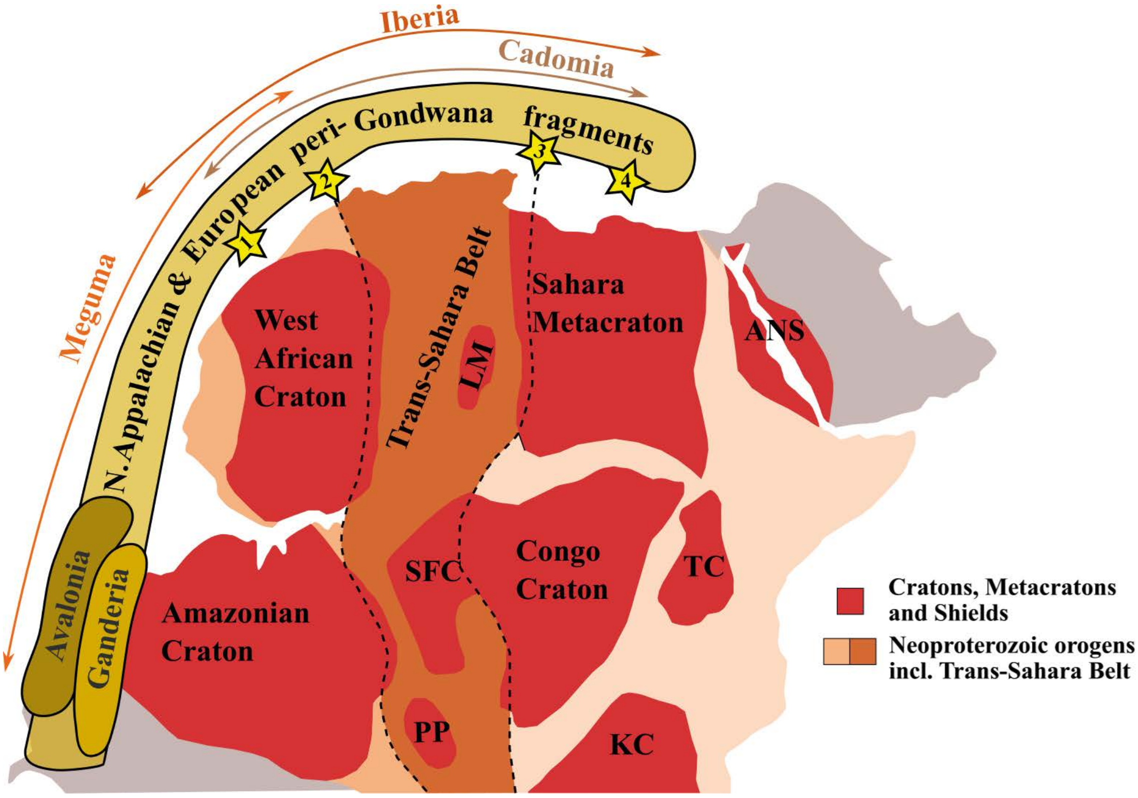

FIGURE 3. Main craton areas, Neoproterozoic orogenic belts in South America and Africa (adapted from Oriolo *et al.*, 2017) and northern Appalachian and European peri-Gondwanan terranes. Numbered stars represent possible paleogeographic settings of 1) Meguma, 2) OMZ, 3) GTMUP, 4) CZ-WALC-CIZ during the EarlyCambrian as depicted by their Birimian-Eburnean distribution (see discussion). Arrows represent the range of paleogeographic settings previously proposed for Neoproterozoic-Cambrian times: Meguma Terrane from West Avalonian (Murphy et al., 2004a) to close to Iberia-Cadomia terranes (Schenk, 1997; White *et al.*, 2018); Iberia terrane(s) from westward of West African Craton (Chichorro *et al.*, 2008) to close to Arabian-Nubian Shield (Cambeses *et al.*, 2017); Cadomian Terranes from northward of West African Craton (Rojo-Pérez *et al.*, 2021) to close to Arabian-Nubian Shield (Couzinié *et al.*, 2019). Avalonia and Ganderia paleographic setting adapted from van Staal *et al.* (2021a). Amazonian Craton (AM); West African Craton (WAC); Trans-Sahara Belt (TSB); Sahara Metacraton (SM); Arabian-Nubian Shield (ANS); LateA Metacraton (LM); São Francisco Craton (SFC); Paranapanema PLate (PP); Congo Craton (CC); Tanzania Craton (TC); Kalahari Craton (KC).

consumption of the Rheic Ocean (Chichorro *et al.*, 2008; Lains Amaral *et al.*, 2022; Linnemann *et al.*, 2008; Mata and Munhá, 1990; Ribeiro *et al.*, 2007; Sánchez-García *et al.*, 2019; Quesada, 2006). It is considered part of the North Gondwana passive margin from the Neoproterozoic to Devonian, as the respective detrital zircon population attest to a typical "West African signature" (*e.g.* Linnemann *et al.*, 2008) and Early Ordovician-Late Devonian rocks contain fauna that suggests a North Gondwana affinity (Robardet and Gutiérrez-Marco, 2004). In the case of the SPZ, its Middle Devonian-Tournaisian rocks have been claimed to have a Laurussia affinity (*e.g.* Ribeiro *et al.*, 2007). Indeed, the palynofloras of the Devonian rocks of its northern sector (PLD) are similar to those found in NW Europe (Pereira *et al.*, 2018), whose affinity to Laurussia is undisputed. More recently, for the IPB (southwards of the PLD), were documented palynozones of key species typical of north Gondwana (Mendes *et al.*, 2018), suggesting a close paleogeographic setting of SPZ and north Gondwana during the Middle Devonian.

The northern domain of SPZ, the PLD (Fig. 2), mainly composed of quartzites and greywackes (Braid *et al.*, 2011; Pereira *et al.*, 2018; Pérez-Cáceres *et al.*, 2017), has been interpreted as an accretionary prism related to subduction under the OMZ (Braid *et al.*, 2010), a Laurussian continental platform unrelated to subduction (Pérez-Cáceres *et al.*, 2020), a Laurussia-derived terrane overlain by a Gondwana-derived accretionary prism related to subduction under the OMZ (Braid *et al.*, 2018) and a back-arc basin related to subduction under the SPZ (Rubio Pascual *et al.*, 2013). Nonetheless, Devonian/Carboniferous? N-MORB metabasalt intercalations in PLD metasediments (ages are highly debatable; see discussion in Pereira *et al.*, 2018) have been identified in northern PLD (Ferreira and Oliveira, 2018; Pérez-Cáceres *et al.*, 2015), supporting a suture zone between the OMZ and SPZ. Furthermore, a narrow heterogeneous oceanic unit (Munhá *et al.*, 1986; Quesada *et al.*, 1994), the Beja-Acebuches Ophiolite Complex, of Carboniferous age (Azor *et al.*, 2008), separates the OMZ and SPZ. This suture is also supported by the occurrence of Ordovician MORBs (interpreted as dismembered ophiolitic slices; Pedro *et al.*, 2010), eclogites (Moita *et al.*, 2005) and other high pressure rocks (Leal *et al.*, 1997) near the southern OMZ border.

In the internal domain of SPZ, IPB (Fig. 2), the lowermost known stratigraphic unit comprises the Phyllite–Quartzite Group (lattermost Famennian in the uppermost section; bottom is currently unknown but at least early Givetian; Mendes *et al.*, 2020), that corresponds to a typical siliciclastic shallow marine environment. The Phyllite–Quartzite Group is divided into the Phyllite–Quartzite Formation and the Barranco do Homem-Represa Formation (Mendes *et al.*, 2018). In the latter, detrital zircon signatures present a critical mid-Late Devonian (Variscan ~390Ma) zircon population (Pereira *et al.*, 2017; Fig. II, Appendix I), whereas such magmatic events are not recorded in the Phyllite–Quartzite Formation sediments (*e.g.* Braid *et al.*, 2011). The Phyllite–Quartzite Group is overlain by the Volcano-Sedimentary Complex, which comprises a Famennian-Tournaisian succession hosting an outstanding volcanogenic massive sulphide (VMS) province, which includes the giant polymetallic sulphide mineralisations of the renowned Neves-Corvo, Aljustrel and Riotinto mines (Lains Amaral *et al.*, 2021b; Leistel *et al.*, 1997; Oliveira *et al.*, 2004; Pereira *et al.*, 2021b; Valenzuela *et al.*, 2011). In the IPB easternmost side, the metamorphosed sedimentary sequences, similar in age to the lower units of the Phyllite-Quartzite Formation (late Givetian-Frasnian?; González *et al.*, 2004), consists of Las Pajanosas and La Minilla units (Matas *et al.*, 2015). In addition, also occurs a Late Devonian sequence, equivalent to the Phyllite-Quartzite Formation (Pérez-Cáceres *et al.*, 2017), the Media Fanega Unit (Simancas, 1983). These are surrounded by the early Carboniferous Sierra Norte Batholith, the largest igneous intrusion of the SPZ (Fig. 2). A Middle Mississippian-Early Pennsylvanian flysch succession, the Baixo Alentejo Flysch Group, overlies the IPB, being interpreted as deposited during the Variscan continental collision (Pereira *et al.*, 2021a; Rodrigues *et al.*, 2015; and references therein).

Considering the relatively enigmatic origin of the SPZ, "missing" a proper old basement, correlations between the SPZ and West Meguma or East Avalonia have been made, in which the latter terranes are thought to have been placed at the border of the Laurussian continent in the Lower Devonian (Braid *et al.*, 2011, 2012; Eden and Andrews, 1990; Franke *et al.*, 2017; Lefort *et al.*, 1988; Pereira *et al.*, 2018; Pérez-Cáceres *et al.*, 2017; von Raumer *et al.*, 2017; de la Rosa *et al.*, 2002; Simancas *et al.*, 2005). In contrast, OMZ has been often correlated with the STZ, both situated in the Gondwana margin throughout the early Paleozoic (Linnemann *et al.*, 2008; Martínez Catalán *et al.*, 2021; Rojo-Pérez *et al.*, 2021). Notwithstanding, recently, White *et al.* (2018) highlighted the detrital zircon similarities between the STZ and West Meguma, suggesting a similar paleogeographic realm in the early Paleozoic.

The known West Meguma comprises a thick turbiditic sequence, the Goldenville Group (uppermost Neoproterozoic?-Cambrian) and the Halifax Group (Lower Ordovician), which is unconformably overlain by a Silurian-Devonian sequence, the Rockville Notch Group (White *et al.*, 2018), interpreted as an overstep (Murphy *et al.*, 2004a) or rift-related sequence (Warsame *et al.*, 2020). The paleogeographic setting of the Meguma terrane has been highly debated, but it has been agreed that Meguma and Avalonia were juxtaposed in the Early Devonian, related to the closure of the Iapetus Ocean and amalgamation of Laurussia (Shellnutt *et al.*, 2019; van Staal *et al.*, 2009). The Meguma terrane is thought to have outboard the Amazonian Craton and been contiguous with West Avalonia in the earliest Paleozoic to later times during the Ordovician-Silurian drifting stage (Murphy *et al.*, 2004a; Shellnutt *et al.*, 2019; Waldron *et al.*, 2009). Indeed, a probable pre-Cambrian Avalonian-type basement for the Meguma terrane has been suggested (Eberz *et al.*, 1991; Greenough *et al.*, 1999). In contrast, it has also been suggested that Meguma was an independent terrane throughout the lower Paleozoic related to the WAC, either or not related to the Amazonian Craton (Schenk, 1997; van Staal *et al.*, 2021a; White *et al.*, 2018).

DATA AND METHODS

The data used in this work was collected from several published works (see Table 1). The U-Pb results gathered from these articles were recalcuLated using the model-2 of Puetz *et al.* (2018) (*i.e.* $^{206}Pb/^{238}U$ age if <1Ga and $^{207}Pb/^{206}Pb$ age if >1Ga), to which was applied a $^{206}Pb/^{238}U$-$^{207}Pb/^{206}Pb$ relative discordance filter of <|10.5|%. Data compiled by Žák *et al.* (2021; Supplemental Table 03) and González Clavijo *et al.* 2021; supplemental table 18) were used without further treatment.

Individual samples Probability Density Plots (PDP) and Kernel Density Estimations (KDE) were performed in the R-package "detzrcr" (Kristoffersen *et al.*, 2015), using a 30Ma bandwidth and a 10Ma size bar (Figs. I-VIII, Appendix I). Multidimensional scaling (MDS) and KDE (30Ma bandwidth) graphs for the datasets (Figs. 4-6; IX-XI) were generated with the R-package 'IsoplotR' (online version) (Vermeesch, 2018). Shepard plot stress values for non-metric Multidimensional scaling yielded a fair-to-good fit (~7-8%) (Kruskal, 1964). In the non-metric Multidimensional scaling graphs (Fig. 4-6), closest neighbour (lines) and second-closest neighbour (dashed-lines) are referred in this work

TABLE 1. Resume of the combined samples used in the present study

Abbreviation used in this study	Atributed age	Tectono-stratigraphic zones / Cratonic areas	Samples	References
OMZ_E	Ediacarian	Ossa-Morena Zone	SNM1, ZD-6, ETZ-32	Pereira *et al.* (2012; Linnemann *et al.* (2008), Fernández-Suárez *et al.* (2002)
OMZ_LC	lower Cambrian	Ossa-Morena Zone	2A-OGL, CTO-33, OLG1, ETZ-30	Linnemann *et al.* (2008), Pereira *et al.* (2011)
OM_MUO	Middle-Upper Ordovician	Ossa-Morena Zone	CH4, Ch3, CH2, EV1, EV2	Azor *et al.* (2021)
IPB_D	Middle-Upper Devonian	Iberian Pyrite Belt	JB-17, SP-114, LR23, RNQ4, RNQ7, RNQ8, RNQ9	Braid *et al.* (2011), Pereira *et al.* (2012), Rosa *et al.* (2008), Pérez-Cáceres *et al.* (2017)
MEG_LC	lower Cambrian	West Meguma	ACO-12-26B, ACO-12-27, LA089, LA090	Henderson *et al.* (2016), Waldron *et al.* (2009)
MEG_MC	middle Cambrian	West Meguma	ACO-12-20B, ACO-12-22A, LA084, LR042	Henderson *et al.* (2016), Waldron *et al.* (2009)
MEG_LO	Lower Ordovician	West Meguma	NB027, LR080B	Pothier *et al.* (2015)
AVL	Ediacaran-Cambrian	West Avalonia	A, B, C, D, E, NB07254A, NB06, AS-86-1, SMB07-117, 10Ca18, 10Ca29, 10Ca43D, 10Ca43C, HMB, ACO-12-29B, ACO-12-38, ACO-12-48, ACO-12-49, ACO-12-50, ACO-12-52a, ACO-12-52b, ACO-12-54, HV95-4, AS06-11	Pollock *et al.* (20090), Barr *et al.* (2012), Willner *et al.* (2013), Murphy *et al.* (2004), Henderson (2016), Satkoski *et al.* (2010)
GAN	Ediacaran-Cambrian	West Ganderia	VL-2001-05, VL-2001-10, VL-2001-03, VL-2001-01, NB11-281, NB10-272, NB12-313, NB16-356, NB16-358	Fyffe *et al.* (2009), Barr *et al.* (2014), Johnson *et al.* (2018), Barr *et al.* (2019)
STZ	Ediacaran-Cambrian	Saxo-Thuringia Zone	C1-Alt-Tb1, C2-Zir1, C3-Katz1, C4-Fro1, C5-LA8-BasQt	Linnemann *et al.* (2014)
LAU	Silurian	East Ganderia	FN033, FN035, LS002A, LS004A, ML109A	Waldron *et al.* (2014)
WAC*	-	West Africa Craton	compiled by Žák *et al.* (2021)	
TSB*	-	Trans-Sahara Belt Belt	compiled by Žák *et al.* (2021)	
SM*	-	Sahara Metacraton	compiled by Žák *et al.* (2021)	
CIZ_E	Ediacaran	Central Iberian Zone	compiled by González Clavijo *et al.* (2021)	
CIZ_LC	lower Cambrian	Central Iberian Zone	compiled by González Clavijo *et al.* (2021)	
CIZ_LO	Lower Ordovician	Central Iberian Zone	compiled by González Clavijo *et al.* (2021)	
WALZCZ_E	Ediacaran	West Asturian–Leonese & Cantabrian zones	compiled by González Clavijo *et al.* (2021)	
WALZCZ_LC	lower Cambrian	West Asturian–Leonese & Cantabrian zones	compiled by González Clavijo *et al.* (2021)	
WALZCZ_LO	Lower Ordovician	West Asturian–Leonese & Cantabrian zones	compiled by González Clavijo *et al.* (2021)	
GMTUP_C	Cambrian	Galicia-Trás-os-Montes upper allochthonous	compiled by González Clavijo *et al.* (2021)	
GMTUP_LO	Lower Ordovician	Galicia-Trás-os-Montes upper allochthonous	compiled by González Clavijo *et al.* (2021)	

*pre-Cambrian igneous and metamorphic zircons

as first-order and second-order relationships. As expected, first- and second-order relationships are identical in both non-metric and classical Multidimensional scaling. Cross-correlation, Likeness, Similarity, Kolmogorov-Smirnov (K-S) Test and Kuiper Test (and D-, V- and p-value) were calculated using Dzstats 2.30 (Saylor and Sundell, 2016) (Table I-III, Electronic Appendix). For Table C, a constant error of 10Ma was used for all terranes.

RESULTS

Below, we describe the combined results of samples grouped by age from the OMZ, West Meguma and IPB detrital lowermost stratigraphic rocks.

Iberian Pyrite Belt: quartzites

For this study, the detrital signature of the quartzites of IPB comprises seven samples, totalling 523 published analyses, 402 of which are concordant. These samples were taken from the Middle-Upper Devonian Phyllite–Quartzite Formation (JB-17 n=61/65; SP-114 n=107/109; LR23 n=8/8) and from Las Pajanosas and La Minilla units (RNQ4 n=57/94; RNQ7 n=56/76; RNQ8 n=61/85; RNQ9 n=52/86; Braid *et al.*, 2011; Pereira *et al.*, 2012a; Pérez-Cáceres *et al.*, 2017; Rosa *et al.*, 2008).

The combined Middle-Upper Devonian samples (JB-17, LR23, SP-114, RNQ4, RNQ7, RNQ8, RNQ9) yield 9 (2%) Lower Devonian-Ordovician grains (406-459Ma), 225 (~56%) Cambrian-lower Tonian grains (500-777Ma), 28 (~7%) middle Tonian-Ectasian (814-1,295Ma), 4 (~1%) Calymmian grains (1,472-1,559Ma), 111 (~28%) Statherian-Rhyacian grains (1,706-2,292Ma), 23 (~6%) Siderian-Archean grains (2,319-3,444Ma). The most probability density peak is at ~598Ma. The Birimian-Eburnean pattern (1.8-2.3Ga; n=103) comprises 30% of Orosirian and 70% of Rhyacian ages (Fig. I).

West Meguma

The peri-Gondwanan detrital signature of the West Meguma terrane is, so far, composed by ten samples, totalling 1,014 published analyses, 638 of which are concordant (Henderson, 2016; Pothier *et al.*, 2015;

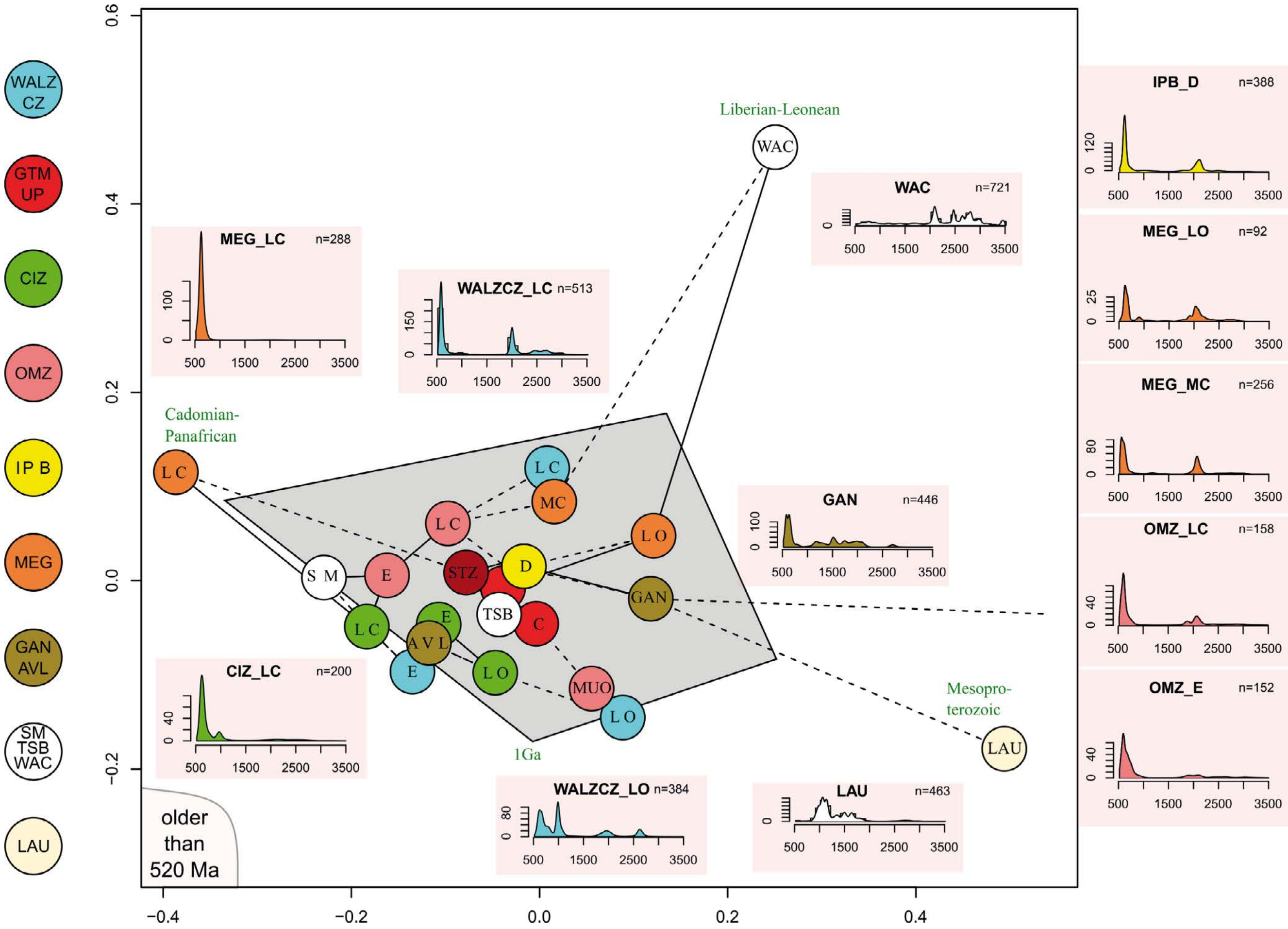

FIGURE 4. Non-metric multidimensional scaling and selected normalized KDE (30Ma bandwith) for analysis older than 520Ma. First-order relationships (line); Second-order relationships (dashedline). WAC: West African Craton (compiled by Žák *et al.*, 2021), TSB: Trans-Saharan Belt (compiled by Žák *et al.*, 2021); SM: Saharan Metacraton (compiled by Žák *et al.*, 2021); STZ: Saxo-Thuringia (Linnemann *et al.*, 2014); LAU: Laurentina signatures of the Silurian East Ganderia sediments (Waldron *et al.*, 2014); CIZ: Central Iberian Zone (compiled by González Clavijo *et al.*, 2021); WALZCZ: West Asturian–Leonese Zone and Cantabrian Zone (compiled by González Clavijo *et al.*, 2021); GTMUP: Galicia–Trás-os-Montes Zone, Upper parautochthon (compiled by González Clavijo *et al.*, 2021); OMZ: Ossa Morena Zone (Fernández-Suárez *et al.*, 2002; Linnemann *et al.*, 2008; Pereira *et al.*, 2011, 2012a); MEG: West Meguma (Henderson, 2016; Pothier *et al.*, 2015; Waldron *et al.*, 2009); IPB: quartzites of the Iberian Pyrite Belt (Braid *et al.*, 2011; Pérez-Cáceres *et al.*, 2017; Pereira *et al.*, 2012b; Rosa *et al.*, 2008); AVL: West Avalonia AVL (Barr *et al.*, 2019; Henderson, 2016; Murphy *et al.*, 2004b; Pollock *et al.*, 2009; Satkoski *et al.*, 2010; Willner *et al.*, 2013); GAN: West Ganderia (Barr *et al.*, 2014, 2019; Fyffe *et al.*, 2009; Johnson *et al.*, 2018). E: Ediacaran; C: Cambrian; LC: Lower Cambrian; MC: Mid Cambrian; LO: Lower Ordovician; MUO: Middle-Upper Ordovician.

Waldron *et al.*, 2009). These samples are from: i) the Goldenville Group (ACO-12-20B n=42/80, ACO-12-22A n=42/80, ACO-12-26B n=53/80, ACO-12-27 n=35/71, LA084 n=47/80, LA089 n=76/85, LA090 n=124/153, LR042=127/142; Henderson *et al.*, 2016; Waldron *et al.*, 2009) and ii) the Halifax Group (NB027 n=43/134, LR080B n=49/109; Pothier *et al.*, 2015).

The combined lower Cambrian samples (ACO-12-27, LAO90, LA089, ACO-12-26B) yield 282 (98%) Cambrian-Tonian grains (525-781Ma; Cambrian n=4, Ediacaran n=169, Cryogenian n=99, Tonian n=10), 1 (~0.5%) Stenian grain (1,004Ma), 4 (1%) Orosirian-Rhyacian grains (1.800-2.065Ma) and 1 (~0.5%) Archean grain (2,794Ma). The most probability density peak is at ~619Ma. The Birimian-Eburnean pattern (1.8-2.3Ga, n=4) comprises 50% of Orosirian and 50% of Rhyacian ages (Fig. III).

The combined middle Cambrian samples (ACO-12-22A, LR042, ACO-12-20B, LA084) yield 135 (~53%) middle Cambrian-lower Tonian grains (505-780Ma), 6 (~2%) middle-upper Tonian grains (838-980Ma), 8 (~3%) Stenian-lowermost Ectasian grains (1,091-1,215Ma), 2 (~1%) Ectasian grains (1,314-1,348Ma), 3 (~1%) Calymmian grains (1,418-1,481Ma), 2 (~1%) Statherian grains (1,719-1,758Ma), 72 (~28%) Orosirian-Rhyacian grains (1,890-2,252Ma), 29 (~11%) Siderian-Archean grains (2,328-3,306Ma). The most significant probability

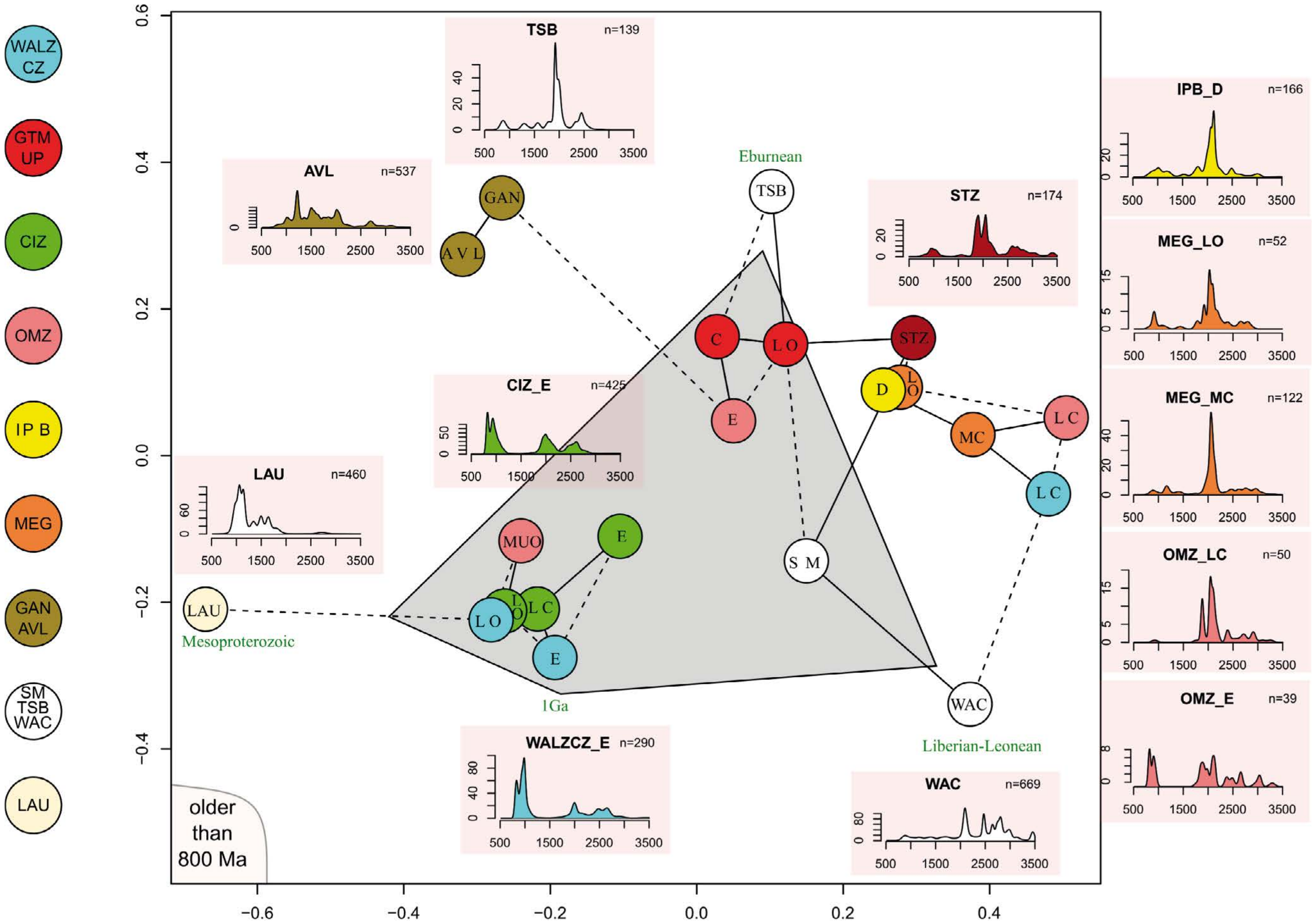

FIGURE 5. Non-metric multidimensional scaling and selected normalised KDE for analysis older than 800Ma. Symbols as in Figure 4.

density peak is at ~549Ma. The Birimian-Eburnean pattern (1.8-2.3Ga, n=72) comprises 35% of Orosirian and 65% of Rhyacian ages (Fig. IV).

The combined Lower Ordovician samples (NB027, LR080B) yield 39 (~42%) Cambrian-Cryogenian grains (512-696Ma; Cambrian n=1; Ediacaran n=19, Cryogenian n=19), 6 (~7%) Tonian grains (734-925Ma), 2 (~2%) Stenian grains (1,016-1,113Ma), 1 (~1%) Calymmian grain (1,430Ma), 2 (~2%) Statherian grains (1,755-1,781Ma), 33 (~36%) Orosirian-Rhyacian grains (1,825-2,299Ma), 3 (~3%) Siderian grains (2,378-2,490Ma) and 6 (~7%) Archean grains (2,610-2,864Ma). The most significant probability density peak is at ~615Ma. The Birimian-Eburnean pattern (1.8-2.3Ga, n=33) comprises 51% of Orosirian and 49% of Rhyacian ages (Fig. V).

Ossa-Morena Zone

Detrital signature of the OMZ comprises seven samples, totalling 1,083 published analyses, 856 of which are concordant (Fernández-Suárez *et al.*, 2002; Linnemann *et al.*, 2008; Pereira *et al.*, 2011, 2012a). These samples are from: i) the Ediacaran formations of the Série Negra succession in the Coimbra–Córdoba Shear Zone (SNM1, n=30/35; Linnemann *et al.*, 2008), Olivenza-Monesterio antiform (ZD-6, n=20/42; Fernández-Suárez *et al.*, 2002) and Estremoz Anticline (ETZ-32, n=103/114; Pereira *et al.* 2012); ii) the lower Cambrian rocks in the Coimbra–Córdoba Shear Zone (2A-OGL, n=27/29; CTO-33, n=28/30; OLG1, n=29/36; Linnemann *et al.*, 2008; Pereira *et al.*, 2011) and Estremoz Anticline (ETZ-30; n=75/77; Pereira *et al.*, 2011) and iii) the Middle-Upper Ordovician rocks from Cerrón del Hornillo and El Valle synclines (CH4, n=117/150; CH3, n=114/150; CH2, n=106/150; EV1, n=113/148; EV2, n=94/122; Azor *et al.*, 2021).

The combined Ediacaran samples (SNM1, ZD-6, ETZ-32) yield 125 (~82%) lowermost Cambrian-Tonian grains (535-946Ma; lowermost Cambrian n=3, Ediacaran n=59, Cryogenian n=33, Tonian n=28); 17 (~11%) late Statherian-Rhyacian grains (1,779-2,147Ma), 4 (~3%) Siderian-lowermost Archean grains (2,364-2,503Ma) and 7 (~5%) Archean grains (2,632-3,292Ma). The most

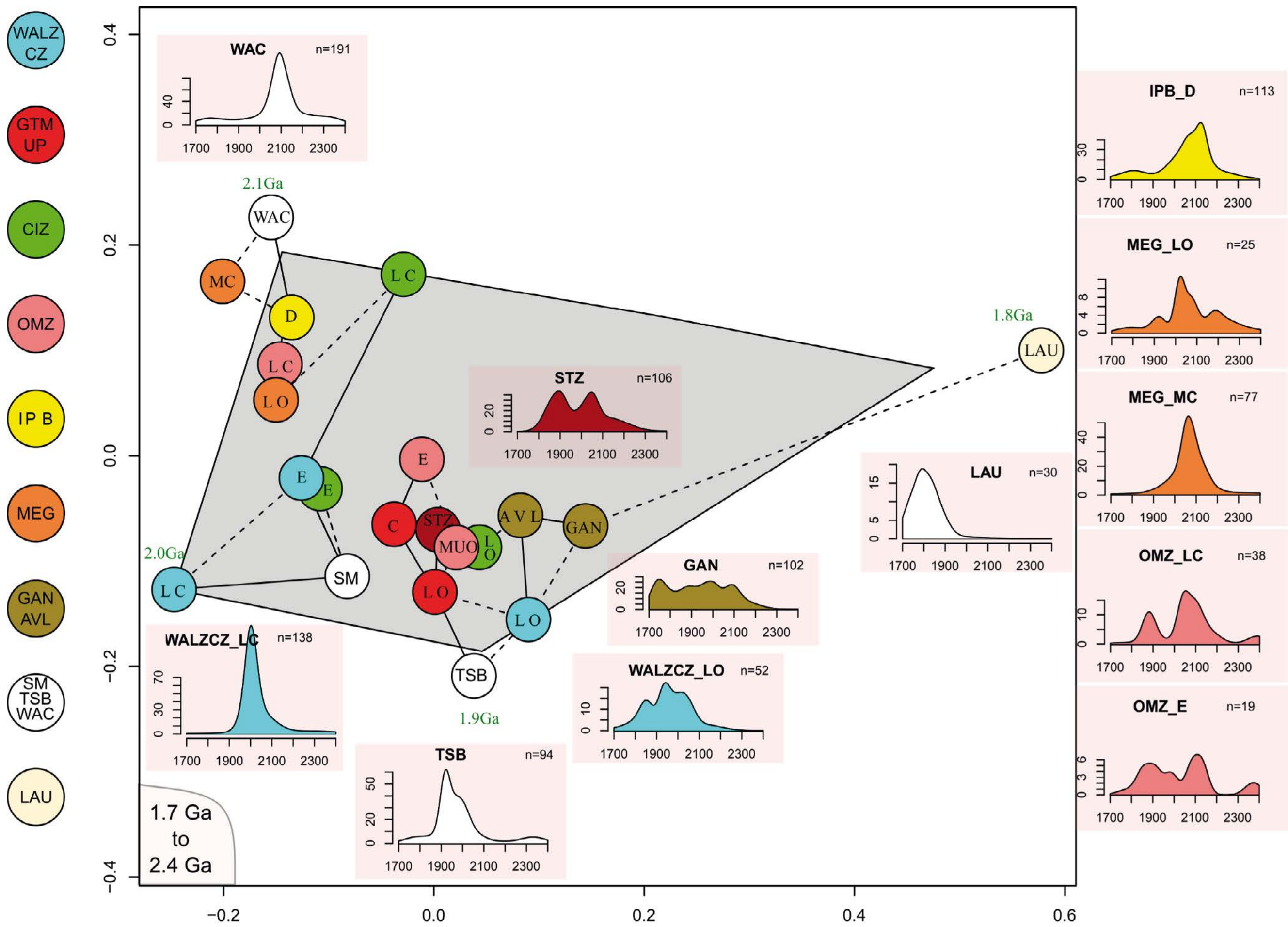

FIGURE 6. Non-metric multidimensional scaling and selected normalised KDE for analysis between 1700 and 2400Ma. Symbols as in Figure 4.

significant probability density peak is at ~594Ma. The Birimian-Eburnean pattern (1.8-2.3Ga, n=16) comprises 56% of Orosirian and 44% of Rhyacian ages (Fig. VI).

The combined lower Cambrian samples (2A-OGL, OLG1, CTO-33, ETZ-30) yield 108 (~68%) lower Cambrian-Tonian grains (532-798Ma; Cambrian n=5, Ediacaran n=70; Cryogenian n=24; Tonian n=9); 1 (~1%) upper Tonian grain (923Ma), 35 (~22%) uppermost Statherian-Rhyacian grains (1,770-2,209Ma) and 14 (~9%) Siderian-Archean grains. The most significant probability density peak is at ~613Ma. The Birimian-Eburnean pattern (1.8-2.3Ga, n=34) comprises 50% of Orosirian and 50% of Rhyacian ages (Fig. VII).

The combined Middle-Upper Ordovician samples (CH4, CH3, CH2, EV1, EV2) yield 8 (~1%) uppermost Cambrian-uppermost Ediacaran grains (487-546Ma); 388 (~71%) Ediacaran-Stenian grains (575-1,124Ma; Ediacaran n=90; Cryogenian n=115; Tonian n=102; Stenian n=81), 16 (~3%) lower Stenian-Calymmian grains (1,178-1,581Ma), 87 (~16%) uppermost Statherian-Rhyacian grains (1.739-2.244Ma), 7 (~1%) Siderian grains (2,324-2,448Ma) and 38 (7%) lowermost Siderian-Archean grains (2,497-3,297Ma). The Birimian-Eburnean pattern (1.8-2.3Ga, n=83) comprises 66% of Orosirian and 44% of Rhyacian ages (Fig. VIII).

DISCUSSION

Full consumption of the Rheic oceanic crust and the onset of the continental collision between OMZ (Gondwana) and SPZ (Laurussia) may have started in the Lower Devonian (Pérez-Cáceres *et al.* 2015; Ribeiro *et al.*, 2007, 2019). Therefore, the two opposing terranes, OMZ and West Meguma are potential detrital zircon sources for the Middle-Upper Devonian quartzites in the Iberian Pyrite Belt.

Braid *et al.* (2011) suggested that the few Mesoproterozoic zircon grains in the IPB, ~5% (Fig. I), indicate a Meguma provenance. However, a dominated Neoproterozoic-Cambrian OMZ source with minor inputs from the sources that provided the “exotic” PLD sediments, characterised by significant Mesoproterozoic fractions, could have originated the observed age patterns of the IPB Devonian rocks. However, these zircon age fractions also could have derived from the Ordovician OMZ rocks, which contain a significant Stenian-Tonian population (Azor *et al.*, 2021; Fig. VIII).

In this section, using visual inspection of the density plots and multidimensional scaling, we will discuss the potential differences between the West Meguma and OMZ Ediacaran-Upper Ordovician rocks, which are the most probable sources for the quartzites of the IPB (without considering the unknown pre-Devonian substrate of the SPZ). In addition, we will address the paleogeographic setting of West Meguma and OMZ during the Cadomian-Panafrican orogeny and subsequent early Paleozoic rifting and drifting.

How similar are IPB, West Meguma and OMZ?

A visual inspection of the PDP and KDE for individual samples of the Ediacaran-Lower Ordovician rocks of OMZ and West Meguma and the Devonian rocks of the IPB suggests a remarkable similarity between these three groups of rocks. Their density patterns are characterised by important Cadomian-Panafrican and Birimian-Eburnean curves and by the paucity of Archean and Mesoproterozoic grains, typical of the so-called "West African signature" (Figs. 4; I-VIII).

Furthermore, statistical analysis suggests remarkable similarities between the IPB (Middle-Upper Devonian), the OMZ (Ediacaran-lower Cambrian) and the West Meguma (middle Cambrian-Lower Ordovician), presenting high Cross-Correlation Coefficients (0.61-0.82), high values of Likeness (0.64-0.73) and Similarity (0.86-0.91). In addition, the K-S test yields D values between 0.13 and 0.21, and the Kuiper test yields V values between 0.17 and 0.26, suggesting that these units are indeed likely close in terms of detrital zircon distribution (Table I).

The statistical resemblance between the IPB and those terranes is better than for the intra-terrane variability of IPB. Indeed, individual samples of the quartzites show worse Cross-Correlation Coefficients (0.59-0.68), Likeness values (0.54-0.62) and Similarity values (0.72-0.81). On the other hand, the K-S and Kuiper tests yield similar values (D-value: 0.16-0.22, V-value: 0-17-0.3, respectively), although p-values are much higher (Table II). These relatively worse values are likely the result of under-represented analyses for each sample (52 to 107 per sample) and highlight the significance of combined detrital zircon age data.

It is interesting the statistical relationship between the lower Cambrian rocks of the OMZ and the middle Cambrian rocks of West Meguma (Table I). They show good Cross-Correlation Coefficients, Likeness values and Similarity values (0.71-0.90). Furthermore, the K-S and Kuiper tests yield 0.16 and 0.23, respectively (Table I). Indeed, the middle Cambrian Meguma is more similar to the lower Cambrian OMZ than any of the other peri-Gondwanan terranes addressed in this work (Table III).

Resemblance with peri-Gondwanan terranes and cratons

In order to assert the resemblance of IPB, West Meguma and OMZ with other peri-Gondwanan terranes and cratons, multidimensional scaling was used to visualise their similarities and dissimilarities.

Devonian, Silurian, Ordovician and upper-middle Cambrian grains in the quartzites of the IPB are rare (~3% altogether). Although their significance cannot be denied, these grains are not relevant for the comparisons addressed in this work. Furthermore, these ages are insignificant in quantity (<<1%) in the other terranes.

Multidimensional scaling for ages older than 520Ma (Fig. 4) presents first-order relationship between IPB Devonian quartzites and Ediacaran-lower Cambrian STZ, Lower Ordovician Galicia-Trás-os-Montes, Upper Parautochthonous (GTMUP) and Ediacaran-Cambrian Ganderia detrital rocks. In addition, it points out the second-order relationship between IPB and Lower Ordovician Meguma and lower Cambrian OMZ. These relationships imply a likely resemblance between the IPB and those terranes. Overall, the IPB is less dissimilar to the TSB than to the WAC and SM. However, an inspection of the combined KDE of the several terranes suggests that the main driver for the observed variations is the relation between the total amount and distribution of Cadomian-Panafrican zircons vs the other fractions, such as the Mesoproterozoic, Paleoproterozoic and Archean zircons (Figs. 4; IX).

For example, the solid Cadomian-Panafrican curve coupled with very few grains older than the Panafrican orogeny (~1%) in the lower Cambrian Meguma rocks represents a kind of end-member for the Cadomian-Panafrican orogeny. In contrast, the WAC end-member represents mainly the Liberian-Leonean influence, and the East Ganderia sediments (Laurentina signatures of the Silurian East Ganderia sediments, Lau) in the Figures 4-6 end-member represents mostly the Mesoproterozoic influence. Another possible end-member is the 1Ga inferred by the prominent peak in the Lower Ordovician rocks of the West Asturian Leonese Zone–Cantabrian Zone (WALZCZ; Figs. 4; IX).

As such, the terranes plotting between the lower Cambrian Meguma and the Lower Ordovician WALZCZ show an increment of the 1Ga fraction relative to the Cadomian-Panafrican curve towards the Lower Ordovician WALZCZ. This feature is observable, for example, in the lower Cambrian CIZ. In the direction of the WAC end-member, the more significant influence of Liberian-Leonean grains in the lower Cambrian WALZCZ relative to the IPB pattern can be observed. On the other hand, the spatial relationship of Avalonia and Ganderia to the other terranes in Figure 4 is more challenging to justify through the aforementioned end-members, which were appropriate for the slight differences among West African-like patterns. To this, it may have contributed the occurrence of Mesoproterozoic and Paleoproterozoic peaks of the same order of magnitude in the Avalonia and Ganderia patterns (Fig. IX), which establishes similarities with other terranes that are not easy to visually explain with the density plots.

In the data compiled by Žák *et al.* (2021) for the pre-Cambrian metamorphic and magmatic zircons of the North African blocks, the TSB represents the typical "West African signature", with solid Cadomian-Panafrican and Birimian-Eburnean curves (Fig. IX). In this respect, the dissimilarities between the Iberian (and Cadomian) sub-terranes are challenging to observe in Figure 4.

Without denying the value of the multidimensional scale for ages older than 520Ma and the Cadomian-Panafrican pattern (*e.g.* Žák *et al.*, 2021; Chichorro *et al.*, 2022, this volume), we evoke that the Cadomian-Panafrican curve, due to its overwhelming relevance, creates a noise factor, diminishing the visual dissimilarities among the peri-Gondwanan terranes in Figure 4. Indeed, we may speculate that the amplitude of the Cadomian-Panafrican curve in the peri-Gondwanan detrital rocks is mainly controlled by the proximity of both (paleo) magmatic arcs (see Chichorro *et al.*, 2022, this volume). Thus, different erosion rates of rocks derived more closely to Cadomian-Panafrican magmatic rocks and of rocks that were least influenced by those magmatic rocks will generate sediments with variable relationships between Cadomian-Panafrican and Birimian-Eburnean curves. An excellent example of such problematic relation is addressed by Zimmermann *et al.* (2015).

By removing the Cadomian-PanAfrican curve (Fig. 5) and considering solely the zircons older than 800Ma, the dissimilarities between the terranes become more evident, although Ediacarian OMZ, lower Cambrian OMZ and Lower Ordovician GTMUP have now few grains (≤50), which may raise a concern about their representativeness (Figs. 5; X). Nonetheless, the multidimensional scaling for ages older than 800Ma indeed separates the peri-Gondwanan terranes into several groups (Fig. 5): i) the Avalonia and Ganderia group, in which both Mesoproterozoic and Birimian-Eburnean fractions are by far the most critical fractions; ii) the WALZCZ (except the lower Cambrian WALZCZ), CIZ and Middle-Upper Ordovician group, is mainly driven by the 1Ga end-member (which in fact represent the overall presence of the 0.85-1.2Ga fractions in these terranes, see, *e.g.* Azor *et al.*, 2021; Henderson *et al.*, 2016); note that the meaning of the first-order relationship of the Laurentia-type sediments with this group is most likely biased, as, for example, the 1.5Ga in the Northern Iberian terranes are poorly represented; iii) the GTMUP and Ediacaran OMZ group, where the 1Ga fraction is still relevant but slightly less than the Birimian-Eburnean fractions; iv) the more extensive group comprising the West Meguma, IPB, lower Cambrian OMZ, lower Cambrian WALZCZ and STZ, in which the Birimian-Eburnean curve is the most crucial feature.

Interesting to note is the first-order relationship of the IPB Devonian rocks with the middle Cambrian and Lower Ordovician rocks of West Meguma, suggesting that West Meguma is the most likely source for the quartzites of the IPB (Fig. 5), as previously suggested by Braid *et al.* (2011). It is also worth noticing the first-order relationship between middle Cambrian Meguma with lower Cambrian OMZ and lower Cambrian WALZCZ (Fig. 5).

Multidimensional scaling vs visual inspection of the Birimian-Eburnean curve

The previous section showed that the multidimensional scaling of filtered data older than the Cadomian-Panafrican curve (*i.e.* >800Ma) could be a powerful tool for discriminating peri-Gondwanan signatures, while the multidimensional scaling including the Cadomian-Panafrican zircons produces less apparent dissimilarities. In this section, we test the multidimensional scaling for ages between 1.7-2.4Ga (Fig. 6) as visual inspection of the Birimian-Eburnean curve suggests relevant differences between the peri-Gondwanan terranes (see below) that may have paleogeographic implications (see next sub-section). Indeed, in the North African cratonic regions, the magmatic and metamorphic events are mainly constrained to ~2.0-2.2Ga in the WAC (Boher *et al.*, 1992; Liégeois *et al.*, 1991; Parra-Avila *et al.*, 2019; Schofield *et al.*, 2006), ~1.9-2.2Ga in the TSB (Bechiri-Benmerzoug *et al.*, 2017; Bendaoud *et al.*, 2008; Nouar *et al.*, 2011; Peucat *et al.*, 2003) and marked by a ~2.0Ga event in the SM (Zhang *et al.*, 2019). Notably, pre-Mesoproterozoic crust is unknown in the Arabian-Nubian Shield (Be'eri-Shlevin *et al.*, 2012; Stern *et al.*, 2010).

Multidimensional scaling of the Birimian-Eburnean ages produces four apparent end-members (Fig. 6): i) the Laurentia-type signatures, with a solid ~1.8Ga peak; ii) the TSB, representing the ~1.9Ga peak; iii) the WALZCZ_LC, marked by a ~2.0Ga prominent peak and iv) the WAC, characterised by a critical ~2.1Ga peak.

The interpretation of the multidimensional scaling also points out the division into three main groups (Fig. 6): i) a group composed of the WAC, IPB, Meguma and lower Cambrian OMZ, in which the 2.1Ga peak is the most important; ii) a group composed of lower Cambrian WALZCZ, Ediacaran WALZCZ, Ediacaran CIZ and SM, marked by a robust 2.0Ga peak, and iii) a more complex group, marked by a strong 1.9Ga peak but as important as other ages. Nonetheless, it is possible to define two main vectors: one towards the WAC composed of GTMUP, STZ, Ediacaran OMZ and Middle-Upper Ordovician OMZ, presenting similar amplitudes of the 1.9 and 2.1Ga peaks and another marked by increasing the 1.7-1.8Ga fraction (Avalonia-Ganderia) and decreasing the 2.1Ga peak (Lower Ordovician WALZCZ -Lower Ordovician CIZ) (Figs. 6; XI).

The Devonian IPB rocks present a first-order relationship with the middle Cambrian Meguma and a second-order relationship with the Lower Ordovician Meguma (Fig. 6), suggesting, once again, that West Meguma is the most suitable terrane to provide zircons to the quartzites of the IPB. Furthermore, the Devonian IPB has a second-order relationship with lower Cambrian OMZ, implying that this terrane could have played a role in forming the Devonian quartzites of the IPB (Fig. 6). However, visual inspection of the Birimian-Eburnean patterns of the IPB, OMZ and West Meguma points out an important distinction between the lower Cambrian OMZ and the Meguma (Fig. 6). As illustrated in the KDE and PDP, the IPB has its main curve between 1.9 and ~2.2Ga, presenting a prominent down peak at ~1.9Ga (Figs. 6; XI). This characteristic is also visible in the middle Cambrian rocks of West Meguma (Figs. 6; IV). On the contrary, the lower Cambrian OMZ is characterised by a prominent 1.9Ga curve with a similar amplitude to the 2.1Ga curve (Figs. 6; VII).

Collectively, multidimensional scaling coupled with a visual inspection of the Birimian-Eburnean pattern strongly suggests that the combined Middle-Upper Devonian IPB quartzites were mainly derived from a middle Cambrian Meguma-type terrane. Nonetheless, the presence of a smooth curve at ~1.8Ga and the Lowermost Devonian-upper Cambrian grains in the Devonian IPB (Fig. I) indicate that other sources were also involved.

Possible paleogeographic implications of the Birimian-Eburnean distribution

Visual inspection of the Birimian-Eburnean distribution (see also Condie *et al.*, 2009) in the WAC, TSB and SM suggests that the specific age frequencies might be helpful for paleogeographic reconstructions of the peri-Gondwanan terranes in Ediacarian Cadomian times and subsequent early Paleozoic rifting and drifting. Indeed, conspicuous peaks at ~2.1Ga for WAC, 1.9Ga for the TSB and ~2.0Ga for the SM (although SM only with 16 analyses; Fig. XI) might have been reflected in late Neoproterozoic-early Phanerozoic peri-Gondwanan sediments. If true, visual inspection of the ages between 1.7 and 2.4Ga in the Ediacaran-Ordovician sediments of the OMZ and West Meguma might help constrain the paleogeography during the Cadomian orogeny, as well as during the Cambrian-Ordovician rift-drift terrane evolution of North Gondwana.

The Late Neoproterozoic-Cambrian paleogeographic relationship of Meguma and OMZ with the WAC has been commonly accepted (Sánchez-García *et al.*, 2019 and references therein). However, paleogeographic reconstructions have placed the OMZ closer to the Cadomian terranes (Chichorro *et al.*, 2008; Linnemann *et al.*, 2008; Rojo-Pérez *et al.*, 2021), in particular, closer to the TSB (Cambeses *et al.*, 2017) or the Anti-Atlas (Linnemann *et al.*, 2008) and placed Meguma between the West African and Amazonian cratons, in particular, in the western (Waldron *et al.*, 2009) or the northern (van Staal *et al.* 2021a, b) North African margins and even adjacent to Avalonia (Murphy *et al.*, 2004). In contrast, Schenk (1997) and White *et al.* (2018) suggested that Meguma was closer to the Iberian and Cadomian terranes (Fig. 3).

The interpretations favoured by Schenk (1997) and Cambeses *et al.* (2017), using stratigraphic correlations and Sm-Nd whole-rock of sediments and detrital U-Pb zircon signatures, are consistent with the Birimian-Eburnean distribution of the Ediacaran-Ordovician sedimentary rocks of West Meguma and OMZ. Indeed, West Meguma middle Cambrian rocks are characterised by a paucity of 1.9Ga ages (Fig. IV), suggesting a WAC derivation (Fig. 6). However, sample LA084 (Waldron *et al.*, 2009) is marked by a slight increment in the 1.9Ga and Tonian-Stenian grains (Fig. IV, note that Puetz *et al.*, 2018 model-2 favours $^{206}Pb/^{238}U$ age over $^{207}Pb/^{206}Pb$, thus removing the "Grenville" grains as reported by Waldron *et al.* 2009), which may suggest the influence of the easternmost North African blocks (TSB and SM). Indeed, Lower Ordovician rocks of Meguma are marked by a relative rise of the 1.9Ga (*e.g.* NB027, Fig. V) and Tonian grains (*e.g.* LR080B, Fig. V), which could suggest an influence of the TSB. On the other hand, the 1.9Ga is very important in the Birimian-Eburnean distribution of the OMZ Ediacaran rocks (Fig. VI), suggesting a strong influence from the TSB. This strong influence is also visible in the lower Cambrian rocks of the OMZ (*e.g.* OLG1, Fig. VII). However, sample ETZ-30, and to a lesser extent sample CTO-33, are marked by the decreasing or absence of the 1.9Ga fractions, suggesting that the TSB source might have been temporarily blocked, which is in accordance with an easternmost position of OMZ relatively to the WAC, as suggested by Cambeses *et al.* (2017) (Fig. 3). Furthermore, these authors suggested that the CIZ and WALZ-CZ were close to the SM (see also *e.g.* Henderson *et al.*, 2016) and the GTMUP were close to both SM and TSB (see also Dias da Silva *et al.*, 2015), which is corroborated by the Birimian-Eburnean distribution of the CIZ-WALZ-CZ Ediacaran-lower Cambrian rocks and GTMUP Cambrian rocks (Figs. 3; 6; XI). The Birimian-Eburnean patterns of the Lower Ordovician rocks of these terranes are diffuser, but that collectively may suggest a westward movement during the Ordovician relatively to their positions in Ediacaran-Cambrian times. In contrast, the eastwards movement of the OMZ (Azor *et al.*, 2021) and possibly Meguma (this work), as inferred by the Tonian-Stenian (Azor *et al.*, 2021) and possibly the 2Ga peaks (Figs. 6; XI) in the Middle-Ordovician OMZ and by 1.9Ga peak in the Lower Ordovician Meguma, suggests that both terranes were in the same fault block in the context of the strike-slip setting that followed the Cadomian subduction (Azor *et al.*, 2021; van Staal *et al.*, 2021a).

Thus, the remarkable similarities between the Ediacarian and early Cambrian OMZ's detrital rocks and the Middle Cambrian and Lower Ordovician rocks of West Meguma (Figs. 4-6; Table I-III), which are much more significant than the similarities to GTMUP-STZ or Avalonia-Ganderia, strongly suggest a (non-contemporaneous) similar paleogeographic setting.

CONCLUSIONS

i) Multidimensional scaling for zircon U-Pb ages older than the Cadomian-Panafrican orogenies (>800Ma) and multidimensional scaling coupled with a visual inspection of the Birimian-Eburnean distribution are powerful tools to discriminate groups and detrital zircon grain provenances of peri-Gondwanan siliciclastic sequences.

ii) Birimian-Eburnean peak distribution 1.8-2.2Ga is an important characteristic to distinguish West Meguma (single peak at ~2.1Ga and trough at 1.9Ga) from Ossa-Morena Zone (identical peaks at 1.9 and 2.1Ga) sources.

iii) The Ediacaran-lower Cambrian detrital rocks of the Ossa-Morena Zone have more remarkable similarities with West Meguma than with other Iberian Massif zones or even with the Saxo-Thuringian Zone, suggesting a close paleogeographic realm.

iv) The Ossa-Morena Zone was close to the Trans-Sahara Belt and West African Craton during the Ediacaran and lower Cambrian, although there might have been temporary shortages of sources from the Trans-Sahara Belt in lower Cambrian times. West Meguma has a great affinity with the West African Craton in the middle Cambrian. In Lower Ordovician times, Meguma might have migrated eastward to a position closer to the Trans-Sahara Belt and Ossa-Morena Zone might have been closer to the Sahara Metacraton.

v) A dominant West Meguma-type provenance (Cambro-Ordovician) for the Middle-Upper Devonian rocks of the Iberian Pyrite Belt is demonstrated, attending to the Birimian-Eburnean pattern similarities and the multidimensional scaling dissimilarities.

vi) The possibility of minor contributions from the Ediacaran-Ordovician rocks of the Ossa-Morena Zone into the Iberian Pyrite Belt quartzites is unlikely, considering the Birimian-Eburnean peak distribution.

ACKNOWLEDGMENTS

We thank Ícaro Dias da Silva and an anonymous reviewer for their constructive comments and suggestions. We also acknowledged Jose Javier Álvaro Blasco and Laura Rincón for editorial handling. We acknowledge the support of FCT through PhD grant SFRH/BD/138791/2018 to João Lains Amaral and through project UIDB/50019/2020 to Instituto Dom Luiz.

REFERENCES

Azor, A., Rubatto, D., Simancas, J.F., González Lodeiro, F., Martínez Poyatos, D., Martín Parra, L.M., Matas, J., 2008. Rheic Ocean ophiolitic remnants in southern Iberia questioned by SHRIMP U-Pb zircon ages on the Beja-Acebuches amphibolites. Tectonics, 27(5), TC5006. DOI: https://doi.org/10.1029/2008TC002306

Azor, A., Martínez Poyatos, D., Accotto, C., Simancas, F., González Lodeiro, F., Talavera, C.,Evans, N.J., 2021. Transcurrent displacement of the Cadomian magmatic arc. Precambrian Research, 361, 106251. DOI: https://doi.org/https://doi.org/10.1016/j.precamres.2021.106251

Barr, S.M., White, C.E., Davis, D.W., McClelland, W.C., van Staal, C.R., 2014. Infrastructure and provenance of Ganderia: Evidence from detrital zircon ages in the Brookville terrane, southern New Brunswick, Canada. Precambrian Research, 246, 358-370. DOI: https://doi.org/https://doi.org/10.1016/j.precamres.2014.03.022

Barr, S.M., van Rooyen, D., Miller, B.V., White, C.E., Johnson, S.C., 2019. Detrital zircon signatures in Precambrian and Paleozoic sedimentary units in Ganderia and Avalonia of southern New Brunswick, Canada – more pieces of the puzzle. Atlantic Geology, 55, 275-322. DOI: https://doi.org/10.4138/atlgeol.2019.010

Be'eri-Shlevin, Y., Eyal, M., Eyal, Y., Whitehouse, M.J., Litvinovsky, B., 2012. The Sa'al volcano-sedimentary complex (Sinai, Egypt): A latest Mesoproterozoic volcanic arc in the northern Arabian Nubian Shield. Geology, 40(5), 403-406. DOI: https://doi.org/10.1130/G32788.1

Bechiri-Benmerzoug, F., Bonin, B., Bechiri, H., Khéloui, R., Talmat-Bouzeguela, S., Bouzid, K., 2017. Hoggar geochronology: a historical review of published isotopic data. Arabian Journal of Geosciences, 10(16), 351. DOI: https://doi.org/10.1007/s12517-017-3134-6

Bendaoud, A., Ouzegane, K., Godard, G., Liégeois, J.-P., Kienast, J.-R., Bruguier, O., Drareni, A., 2008. Geochronology and metamorphic P-T-X evolution of the Eburnean granulite-facies metapelites of Tidjenouine (Central Hoggar, Algeria): Witness of the latea metacratonic evolution. London, The Geological Society, 297(1, Special Publications), 111-146. DOI: https://doi.org/10.1144/SP297.6

Boher, M., Abouchami, W., Michard, A., Albarede, F., Arndt, N.T., 1992. Crustal growth in West Africa at 2.1 Ga. Journal of Geophysical Research: Solid Earth, 97(B1), 345-369. DOI: https://doi.org/https://doi.org/10.1029/91JB01640

Braid, J.A., Murphy, J.B., Quesada, C., 2010. Structural analysis of an accretionary prism in a continental collisional setting, the Late Paleozoic Pulo do Lobo Zone, Southern Iberia. Gondwana Research, 17(2-3), 422-439. DOI: https://doi.org/10.1016/J.GR.2009.09.003

Braid, J.A., Murphy, J.B., Quesada, C., Mortensen, J., 2011. Tectonic escape of a crustal fragment during the closure of the Rheic Ocean: U–Pb detrital zircon data from the Late Palaeozoic Pulo do Lobo and South Portuguese zones, southern Iberia. Journal of the Geological Society, 168(2), 383-392. DOI: https://doi.org/10.1144/0016-76492010-104

Braid, J.A., Murphy, J.B., Quesada, C., Bickerton, L., Mortensen, J.K., 2012. Probing the composition of unexposed basement, South Portuguese Zone, southern Iberia: Implications for the connections between the Appalachian and Variscan orogens. Canadian Journal of Earth Sciences, 49(4), 591-613. DOI: https://doi.org/10.1139/E11-071

Braid, J.A., Murphy, J.B., Quesada, C., Gladney, E.R., Dupuis, N., 2018. Progressive magmatism and evolution of the Variscan suture in southern Iberia. International Journal of Earth Sciences, 107, 971-983. DOI: https://doi.org/https://doi.org/10.1007/s00531-017-1540-3

Cambeses, A., Scarrow, J.H., Montero, P., Lázaro, C., Bea, F., 2017. Palaeogeography and crustal evolution of the Ossa–Morena Zone, southwest Iberia, and the North Gondwana margin during the Cambro-Ordovician: a review of isotopic evidence. International Geology Review, 59(1), 94-130. DOI: https://doi.org/10.1080/00206814.2016.1219279

Chichorro, M., Pereira, M.F., Díaz-Azpiroz, M., Williams, I.S., Fernández, C., Pin, C., Silva, J.B., 2008. Cambrian ensialic rift-related magmatism in the Ossa-Morena Zone (Évora–Aracena metamorphic belt, SW Iberian Massif): Sm–Nd isotopes and SHRIMP zircon U–Th–Pb geochronology. Tectonophysics, 461(1), 91-113. DOI: https://doi.org/https://doi.org/10.1016/j.tecto.2008.01.008

Chichorro, M., Solá, R., Bento dos Santos, T.M., Lains Amaral, J., Crespin, L., 2022. Tracking the Cadomian/Pan-African consolidation of the Iberian Massif by its detrital and inherited zircon populations: is the ~610 Ma age peak a prolonged Cadomian magmatism inheritance or the key to unravel its Pan-African basement? Geologia Acta, 20.15, 1-29.

Condie, K.C., Belousova, E., Griffin, W.L., Sircombe, K.N., 2009. Granitoid events in space and time: Constraints from igneous and detrital zircon age spectra. Gondwana Research, 15(3), 228-242. DOI: https://doi.org/https://doi.org/10.1016/j.gr.2008.06.001

Couzinié, S., Laurent, O., Chelle-Michou, C., Bouilhol, P., Paquette, J.-L., Gannoun, A.-M., Moyen, J.-F., 2019. Detrital zircon U–Pb–Hf systematics of Ediacaran metasediments from the French Massif Central: Consequences for the crustal evolution of the north Gondwana margin. Precambrian Research, 324, 269-284. DOI: https://doi.org/https://doi.org/10.1016/j.precamres.2019.01.016

Dias da Silva, Í., Linnemann, U., Hofmann, M., González-Clavijo, E., Díez-Montes, A., Martínez Catalán, J.R., 2015. Detrital zircon and tectonostratigraphy of the Parautochthon under the Morais Complex (NE Portugal): implications for the Variscan accretionary history of the Iberian Massif. Journal of the Geological Society, 172(1), 45-61. DOI: https://doi.org/10.1144/jgs2014-005

Eberz, G.W., Clarke, D.B., Chatterjee, A.K., Giles, P.S., 1991. Chemical and isotopic composition of the Lower crust beneath the Meguma Lithotectonic Zone, Nova Scotia: evidence from granulite facies xenoliths. Contributions to Mineralogy and Petrology, 109(1), 69-88. DOI: https://doi.org/10.1007/BF00687201

Eden, C.P., Andrews, J.R., 1990. Middle to upper Devonian melanges in SW Spain and their relationship to the Meneage Formation in south Cornwall. Proceedings of the Ussher Society, 7, 217-222.

Farias, P., Gallastegui, G., González Lodeiro, F., Marquínez, J., Martín Parra, L.M., Martínez Catalán, J.R., de Pablo Maciá, J.G., Rodríguez Fernández, L.R., 1987. Aportaciones al conocimiento de la litoestratigrafía y estructura de Galicia Central. Memórias da Faculdade de Ciências, Universidade do Porto, 1, 411-431.

Fernández-Suárez, J., Gutiérrez Alonso, G., Jeffries, T.E., 2002. The importance of along-margin terrane transport in northern Gondwana: insights from detrital zircon parentage in Neoproterozoic rocks from Iberia and Brittany. Earth and Planetary Science Letters, 204(1), 75-88. DOI: https://doi.org/https://doi.org/10.1016/S0012-821X(02)00963-9

Ferreira, P.L. Oliveira, J.T., 2018. Geochemical characteristics of Pulo do Lobo metabasalts from ALF-2 drill core, SE of Trindade village, Alentejo, Portugal. Actas of the XIV Congresso de Geoquímica dos Países de Língua Portuguesa e XIX Semana de Geoquímica, 5pp.

Franke, W., Cocks, L.R.M., Torsvik, T.H., 2017. The Palaeozoic Variscan oceans revisited. Gondwana Research, 48, 257-284. DOI: https://doi.org/https://doi.org/10.1016/j.gr.2017.03.005

Fyffe, L.R., Barr, S.M., Johnson, S.C., McLeod, M.J., McNicoll, V.J., Valverde-Vaquero, P., Van Staal, C.R., White, C.E., 2009. Detrital zircon ages from Neoproterozoic and early Paleozoic conglomerate and sandstone units of New Brunswick and coastal Maine: implications for the tectonic evolution of Ganderia. Atlantic Geology, 45, 110-144. DOI: https://doi.org/https://doi.org/10.4138/atlgeol.2009.006

González, F., Moreno, C., López, M.J., Dino, R., Antonioli, L., 2004. Palinoestratigrafía del Grupo Pizarroso-Cuarcítico del sector más oriental de la Faja Pirítica Ibérica, SO de España. Revista Española de Micropaleontología, 36(2), 279-304.

González Clavijo, E., Dias da Silva, Í., Martínez Catalán, J.R., Gómez Barreiro, J., Gutiérrez-Alonso, G., Díez Montes, A., Hofmann, M., Gärtner, A., Linnemann, U., 2021. A tectonic carpet of Variscan flysch at the base of a rootless accretionary prism in northwestern Iberia: U–Pb zircon age constrains from sediments and volcanic olistoliths. Solid Earth, 12(4), 835-867. DOI: https://doi.org/https://doi.org/10.5194/se-12-835-2021

Greenough, J.D., Krogh, T.E., Kamo, S.L., Owen, J.V., Ruffman, A., 1999. Precise U-Pb dating of Meguma basement xenoliths: new evidence for Avalonian underthrusting. Canadian Journal of Earth Sciences, 36(1), 15-22. DOI: https://doi.org/10.1139/e98-079

Henderson, B.J., 2016. What do epsilon hafnium isotopic arrays tell us about Wilson cycle tectonics? implications for the type area in the Appalachian-Variscan Orogen. Doctoral Thesis. Adelaide (Australia), University of Adelaide, unpublished, 340pp. DOI: https://doi.org/10.4225/55/5a20e844ea4ea

Henderson, B.J., Collins, W.J., Murphy, J.B., Gutierrez-Alonso, G., Hand, M., 2016. Gondwanan basement terranes of the Variscan–Appalachian orogen: Baltican, Saharan and West African hafnium isotopic fingerprints in Avalonia, Iberia and the Armorican Terranes. Tectonophysics, 681, 278-304. DOI: https://doi.org/https://doi.org/10.1016/j.tecto.2015.11.020

Johnson, S.C., Dunning, G.R., Miller, B.V., 2018. U-Pb geochronology and geochemistry from the northeastern New River belt, southern New Brunswick, Canada: significance of the Almond Road Group to the Ganderian platformal margin. Atlantic Geology, 54, 147-170. DOI: https://doi.org/https://doi.org/10.4138/atlgeol.2018.005

Julivert, M., Fontboté, J. M., Ribeiro, A., Conde, L., 1974. Memoria explicativa del Mapa Tectónico de la Peninsula Ibérica y Baleares. Madrid, Instituto Geologico y Minero de España (IGME), 1:1,000,000, 1-101.

Kristoffersen, M., Andersen, T., Elburg, M.A., Watkeys, M.K., 2015. Detrital zircon in a supercontinental setting: locally derived and far-transported components in the Ordovician Natal Group, South Africa. Journal of the Geological Society, 173(1), 203-215. DOI: https://doi.org/10.1144/jgs2015-012

Kruskal, J.B., 1964. Multidimensional scaling by optimizing goodness of fit to a nonmetric hypothesis. Psychometrika, 29(1), 1-27. DOI: https://doi.org/10.1007/BF02289565

Lains Amaral, J., Solá, A., Bento dos Santos, T., 2021a. Inspecting zircon populations of the Iberian Pyrite Belt: tracking the Cadomian record of the South Portuguese Zone. In: Álvaro, J.J., Chichorro, M., Gutiérrez-Alonso G. (eds.). The Panafrican and Cadomian orogenies in North Africa and Western Europe. Madrid, IGEO ed., 8. DOI: https://doi.org/10.5281/ZENODO.5084628

Lains Amaral, J., Solá, A.R., Bento dos Santos, T.M., Tassinari, C.C.G., Gonçalves, J., 2021b. U-Pb zircon SHRIMP dating of a protracted magmatic setting and its volcanic emplacement: insights from the felsic volcanic rocks hosting the sulphide ore of the giant Aljustrel Deposit, Iberian Pyrite Belt. Ore Geology Reviews, 134, 104147. DOI: https://doi.org/https://doi.org/10.1016/j.oregeorev.2021.104147

Lains Amaral, J., Mata, Santos, J.F., 2022. The Carboniferous shoshonitic (s.l.) gabbro–monzonitic stocks of Veiros and Vale de Maceira, Ossa-Morena Zone (SW Iberian Massif): Evidence for diverse subduction-related lithospheric metasomatism. Geochemistry, 82(4), 125917. DOI: https://doi.org/10.1016/j.chemer.2022.125917

Leal, N., Pedro, J., Moita, P., Fonseca, P., Araújo, A., Munhá, J., 1997. Metamorfismo nos sectores meridionais da Zona de Ossa-Morena: Actualização dos Conhecimentos. In: Araújo, A., Pereira, M.F. (eds). Estudos sobre a Geologia da Zona de Ossa Morena (Maciço Ibérico). Livro de Homenagem ao Prof. Francisco Gonçalves, Universidade de Évora, 119-132.

Lefort, J.P., Max, M.D., Roussel, J., 1988. Geophysical evidence for the location of the NW boundary of Gondwanaland and its relationship with two older satellite sutures. London, The Geological Society, 38(1, Special Publications), 49-60. DOI: https://doi.org/10.1144/GSL.SP.1988.038.01.04

Leistel, J.M., Marcoux, E., Thiéblemont, D., Quesada, C., Sánchez, A., Almodóvar, G.R., Pascual, E., Sáez, R., 1997. The volcanic-hosted massive sulphide deposits of the Iberian Pyrite Belt. Mineralium Deposita, 33(1-2), 2-30. DOI: https://doi.org/10.1007/s001260050130

Liégeois, J.P., Claessens, W., Camara, D., Klerkx, J., 1991. Short-lived Eburnian orogeny in southern Mali. Geology, tectonics, U-Pb and Rb-Sr geochronology. Precambrian Research, 50(1), 111-136. DOI: https://doi.org/https://doi.org/10.1016/0301-9268(91)90050-K

Linnemann, U., Pereira, F., Jeffries, T.E., Drost, K., Gerdes, A., 2008. The Cadomian Orogeny and the opening of the Rheic Ocean: The diacrony of geotectonic processes constrained by LA-ICP-MS U–Pb zircon dating (Ossa-Morena and Saxo-Thuringian Zones, Iberian and Bohemian Massifs). Tectonophysics, 461(1), 21-43. DOI: https://doi.org/https://doi.org/10.1016/j.tecto.2008.05.002

Linnemann, U., Gerdes, A., Hofmann, M., Marko, L., 2014. The Cadomian Orogen: Neoproterozoic to Early Cambrian crustal growth and orogenic zoning along the periphery of the West African Craton—Constraints from U–Pb zircon ages and Hf isotopes (Schwarzburg Antiform, Germany). Precambrian Research, 244, 236-278. DOI: https://doi.org/https://doi.org/10.1016/j.precamres.2013.08.007

Lotze, F., 1945. Zur gliederung der Varisziden der Iberischru Meseta. Geotektonische Forschungen, 6, 78-92.

Martínez Catalán, J.R., Schulmann, K., Ghienne, J.-F., 2021. The Mid-Variscan Allochthon: Keys from correlation, partial retrodeformation and plate-tectonic reconstruction to unlock the geometry of a non-cylindrical belt. Earth-Science Reviews, 220, 103700. DOI: https://doi.org/10.1016/j.earscirev.2021.103700

Mata, J., Munhá, J., 1990. Magmatogénese de metavulcanitos câmbricos do nordeste alentejano: os estádios iniciais de "rifting" continental. Comunicacões dos Servicos Geológicos de Portugal, 76, 61-89.

Matas, J., Martín Parra, L.M., Rubio Pascual, F., 2015. Mapa Geológico de España 1: 200.000, sheet 75/74: Sevilla-Puebla de Guzmán, Instituto Geologico y Minero de España (IGME).

Mendes, M., Pereira, Z., Matos, J.X., Albardeiro, L., Morais, I., Solá, R., Pacheco, N., Araújo, V., 2018. Middle-Upper Devonian Palynostratigraphy of the Phyllite-Quartzite Group. The Neves-Corvo Mine Region, Iberian Pyrite Belt - Correlation with The South Portuguese Zone. In: Vaz, N., Sá, A.A. (eds.). Yacimientos paleontológicos excepcionales en la Península Ibérica. Madrid, Instituto Geológico y Minero de España (IGME), Cuadernos del Museo Geominero, 357-365.

Mendes, M., Pereira, Z., Matos, J.X., Albardeiro, L., Morais, I., Solá, R., Salgueiro, R., Pacheco, N., Araújo, V., Inverno, C., Oliveira, J.T., 2020. New insights on the middle Givetian/ middle Frasnian palynofloras from the Phyllite-Quartzite Formation in the Neves-Corvo mine region (Iberian Pyrite Belt, Portugal). Revue de Micropaléontologie, 68, 100447. DOI: https://doi.org/10.1016/j.revmic.2020.100447

Moita, P., Munhá, J., Fonseca, P., Pedro, J., Araújo, A., Tassinari, C., Palacios, T., 2005. Phase equilibria and geochronology of Ossa-Morena eclogites. Actas of the XIV Semana de Geoquímica/VIII Congresso de Geoquímica dos Países de Língua Portuguesa, 463-466.

Munhá, J., Oliveira, J.T., Ribeiro, A., Oliveira, V., Quesada, C., Kerrich, R., 1986. Beja-Acebuches Ophiolite characterization and geodynamic significance. Maleo, 2(13), 31.

Murphy, J.B., Fernández-Suárez, J., Keppie, J.D., Jeffries, T.E., 2004a. Contiguous rather than discrete Paleozoic histories for the Avalon and Meguma terranes based on detrital zircon data. Geology, 32(7), 585-588. DOI: https://doi.org/10.1130/G20351.1

Murphy, J.B., Fernández-Suárez, J., Jeffries, T., Strachan, R., 2004b. U–Pb (LA–ICP-MS) dating of detrital zircons from Cambrian clastic rocks in Avalonia: erosion of a Neoproterozoic arc along the northern Gondwanan margin. Journal of the Geological Society, 161(2), 243-254. DOI: https://doi.org/10.1144/0016-764903-064

Nouar, O., Henry, B., Liégeois, J.P., Derder, M.E.M., Bayou, B., Bruguier, O., Ouabadi, A., Amenna, M., Hemmi, A., Ayache, M., 2011. Eburnean and Pan-African granitoids and the Raghane mega-shear zone evolution: Image analysis, U–Pb zircon age and AMS study in the Arokam Ténéré (Tuareg shield, Algeria). Journal of African Earth Sciences, 60(3), 133-152. DOI: https://doi.org/https://doi.org/10.1016/j.jafrearsci.2011.02.007

Oliveira, J.T., Pereira, Z., Carvalho, P., Pacheco, N., Korn, D., 2004. Stratigraphy of the tectonically imbricated lithological succession of the Neves Corvo mine area, Iberian Pyrite Belt, Portugal. Mineralium Deposita, 39(4), 422-436. DOI: https://doi.org/10.1007/s00126-004-0415-2

Oliveira, J.T., Relvas, J., Pereira, Z., Munhá, J., Rosa, C., Rosa, D., Fernandes, P., Jorge, R., Pinto, Á., 2013. Geologia Sul Portuguesa, com ênfase na estratigrafia, vulcanologia física, geoquímica e mineralizações da faixa piritosa, In: Dias, R., Araújo, A., Terrinha, P., Kullberg, J.C. (eds.). Geologia Pré-mesozóica de Portugal. Escolar editora, 1, 673-765.

Oliveira, J.T., 2015. História das contribuições científicas originais que representam avanços significativos no contexto do conhecimento tectono-estratigráfico da Zona Sul Portuguesa, em Portugal. Geonovas, 28, 3-21.

Oliveira, J.T., Quesada, C., Pereira, Z., Matos, J.X., Solá, A.R., Rosa, D., Albardeiro, L., Díez-Montes, A., Morais, I., Inverno, C., Rosa, C., Relvas, J., 2019. South Portuguese Terrane: A Continental Affinity Exotic Unit. In: Quesada, C., Oliveira, J.T. (eds.). The Geology of Iberia: A Geodynamic Approach. The Variscan Cycle. Regional Geology Review, Springer Cham, 173-206. DOI: https://doi.org/10.1007/978-3-030-10519-8_6

Oriolo, S., Oyhantçabal, P., Wemmer, K., Siegesmund, S., 2017. Contemporaneous assembly of Western Gondwana and final Rodinia break-up: Implications for the supercontinent cycle. Geoscience Frontiers, 8(6), 1431-1445. DOI: https://doi.org/https://doi.org/10.1016/j.gsf.2017.01.009

Parra-Avila, L.A., Baratoux, L., Eglinger, A., Fiorentini, M.L., Block, S., 2019. The Eburnean magmatic evolution across the Baoulé-Mossi domain: Geodynamic implications for the West African Craton. Precambrian Research, 332, 105392. DOI: https://doi.org/https://doi.org/10.1016/j.precamres.2019.105392

Pedro, J.C., Araújo, A., Fonseca, P., Tassinari, C., Ribeiro, A., 2010. Geochemistry and U-Pb zircon age of the internal Ossa-Morena Zone ophiolite sequences: a remnant of Rheic Ocean in SW Iberia. Ofioliti, 35(2), 117-130. DOI: https://doi.org/10.4454/ofioliti.v35i2.390

Pereira, M.F., Chichorro, M., Solá, A.R., Silva, J.B., Sánchez-García, T., Bellido, F., 2011. Tracing the Cadomian magmatism with detrital/inherited zircon ages by in-situ U–Pb SHRIMP geochronology (Ossa-Morena Zone, SW Iberian Massif). Lithos, 123(1), 204-217. DOI: https://doi.org/https://doi.org/10.1016/j.lithos.2010.11.008

Pereira, M.F., Solá, A.R., Chichorro, M., Lopes, L., Gerdes, A., Silva, J.B., 2012a. North-Gondwana assembly, break-up and paleogeography: U–Pb isotope evidence from detrital and igneous zircons of Ediacaran and Cambrian rocks of SW Iberia. Gondwana Research, 22(3-4), 866-881. DOI: https://doi.org/10.1016/J.GR.2012.02.010

Pereira, M.F., Chichorro, M., Johnston, S.T., Gutiérrez-Alonso, G., Silva, J.B., Linnemann, U., Hofmann, M., Drost, K., 2012b. The missing Rheic Ocean magmatic arcs: Provenance analysis of Late Paleozoic sedimentary clastic rocks of SW Iberia. Gondwana Research, 22(3-4), 882-891. DOI: https://doi.org/https://doi.org/10.1016/j.gr.2012.03.010

Pereira, M.F., Gutíerrez-Alonso, G., Murphy, J.B., Drost, K., Gama, C., Silva, J.B., 2017. Birth and demise of the Rheic Ocean magmatic arc(s): Combined U–Pb and Hf isotope analyses in detrital zircon from SW Iberia siliciclastic strata.

Lithos, 278-281, 383-399. DOI: https://doi.org/10.1016/j.lithos.2017.02.009

Pereira, Z., Fernandes, P., Matos, J.X., Jorge, R.C.G.S., Oliveira, J.T., 2018. Stratigraphy of the Northern Pulo do Lobo Domain, SW Iberia Variscides: A palynological contribution. Geobios, 51(6), 491-506. DOI: https://doi.org/10.1016/j.geobios.2018.04.001

Pereira, M.F., Gama, C., Dias da Silva, Í., Fuenlabrada, J.M., Silva, J.B., Medina, J., 2021a. Isotope geochemistry evidence for Laurussian-type sources of South Portuguese Zone Carboniferous turbidites (Variscan Orogeny). London, The Geological Society, 503(1, Special Publications), 619-642. DOI: https://doi.org/10.1144/SP503-2019-163

Pereira, Z., Matos, J.X., Solá, A.R., Batista, M.J., Salgueiro, R., Rosa, C., Albardeiro, L., Mendes, M., Morais, I., de Oliveira, D., Pacheco, N., Araújo, V., Castelo Branco, J.M., Neto, R., Lains Amaral, J., Inverno, C., Oliveira, J.T., 2021b. Geology of the recently discovered massive and stockwork sulphide mineralization at Semblana, Rosa Magra and Monte Branco, Neves–Corvo mine region, Iberian Pyrite Belt, Portugal. Geological Magazine, 158(7), 1-16. DOI: https://doi.org/DOI: 10.1017/S0016756820001284

Pérez-Cáceres, I., Martínez Poyatos, D., Simancas, J.F., Azor, A., 2015. The elusive nature of the Rheic Ocean suture in SW Iberia. Tectonics, 34, 2429-2450.

Pérez-Cáceres, I., Martínez Poyatos, D., Simancas, J.F., Azor, A., 2017. Testing the Avalonian affinity of the South Portuguese Zone and the Neoproterozoic evolution of SW Iberia through detrital zircon populations. Gondwana Research, 42, 177-192. DOI: https://doi.org/10.1016/J.GR.2016.10.010

Pérez-Cáceres, I., Martínez Poyatos, D.J., Vidal, O., Beyssac, O., Nieto, F., Simancas, J.F., Azor, A., Bourdelle, F., 2020. Deciphering the metamorphic evolution of the Pulo do Lobo metasedimentary domain (SW Iberian Variscides). Solid Earth, 11(2), 469-488. DOI: https://doi.org/10.5194/se-11-469-2020

Peucat, J.J., Drareni, A., Latouche, L., Deloule, E., Vidal, P., 2003. U–Pb zircon (TIMS and SIMS) and Sm–Nd whole-rock geochronology of the Gour Oumelalen granulitic basement, Hoggar massif, Tuareg shield, Algeria. Journal of African Earth Sciences, 37(3), 229-239. DOI: https://doi.org/https://doi.org/10.1016/j.jafrearsci.2003.03.001

Pollock, J.C., Hibbard, J.P., Sylvester, P.J., 2009. Early Ordovician rifting of Avalonia and birth of the Rheic Ocean: U–Pb detrital zircon constraints from Newfoundland. Journal of the Geological Society, 166(3), 501-515. DOI: https://doi.org/10.1144/0016-76492008-088

Pothier, H.D., Waldron, J.W.F., Schofield, D.I., DuFrane, S.A., 2015. Peri-Gondwanan terrane interactions recorded in the Cambrian-Ordovician detrital zircon geochronology of North Wales. Gondwana Research, 28(3), 987-1001. DOI: https://doi.org/10.1016/j.gr.2014.08.009

Puetz, S.J., Ganade, C.E., Zimmermann, U., Borchardt, G., 2018. Statistical analyses of Global U-Pb Database 2017. Geoscience Frontiers, 9(1), 121-145. DOI: https://doi.org/10.1016/J.GSF.2017.06.001

Quesada, C., Fonseca, P.E., Munhá, J., Oliveira, J.T., Ribeiro, A., 1994. The Beja-Acebuches Ophiolite (Southern iberia Variscan Fold Belt): geological characterization and geodynamic significance. Boletín Geológico y Minero, 105(1), 3-49.

Quesada, C., 2006. The Ossa-Morena Zone of the Iberian Massif: a tectonostratigraphic approach to its evolution. Zeitschrift der Deutschen Gesellschaft für Geowissenschaften, 157(4), 585-595. DOI: https://doi.org/10.1127/1860-1804/2006/0157-0585

von Raumer, J.F., Nesbor, H.-D., Stampfli, G.M., 2017. The north-subducting Rheic Ocean during the Devonian: consequences for the Rhenohercynian ore sites. International Journal of Earth Sciences, 106(7), 2279-2296. DOI: https://doi.org/10.1007/s00531-016-1425-x

Ribeiro, A., Munhá, J., Dias, R., Mateus, A., Pereira, E., Ribeiro, L., Fonseca, P., Araújo, A., Oliveira, T., Romão, J., 2007. Geodynamic evolution of the SW Europe Variscides. Tectonics, 26(6), TC6009. DOI: https://doi.org/10.1029/2006TC002058

Ribeiro, M.L., Castro, A., Almeida, A., Menéndez, L.G., Jesus, A., Lains Amaral, J., Lopes, J.C., Martins, H.C.B., Mata, J., Mateus, A., Moita, P., Neiva, A.M.R., Ribeiro, M.A., Santos, J.F., Solá, A.R., 2019. Variscan Magmatism. In: Quesada, C., Oliveira, J.T. (eds.). The Geology of Iberia: A Geodynamic Approach: The Variscan Cycle. Regional Geology Review, Springer Cham, 497-526. DOI: https://doi.org/10.1007/978-3-030-10519-8_13

Robardet, M., 2003. The Armorica “microplate”: Fact or fiction? Critical review of the concept and contradictory palaeobiogeographical data. Palaeogeography, Palaeoclimatology, Palaeoecology, 195(1-2), 125-148. DOI: https://doi.org/10.1016/S0031-0182(03)00305-5

Robardet, M., Gutiérrez-Marco, J.C., 2004. The Ordovician, Silurian and Devonian sedimentary rocks of the Ossa-Morena Zone (SW Iberian Peninsula, Spain). Journal of Iberian Geology, 30, 73-92.

Rodrigues, B., Chew, D.M., Jorge, R.C.G.S., Fernandes, P., Veiga-Pires, C., Oliveira, J.T., 2015. Detrital zircon geochronology of the Carboniferous Baixo Alentejo Flysch Group (South Portugal); constraints on the provenance and geodynamic evolution of the South Portuguese Zone. Journal of the Geological Society, 172(3), 294-308. DOI: https://doi.org/10.1144/jgs2013-084

Rojo-Pérez, E., Fuenlabrada, J.M., Linnemann, U., Arenas, R., Sánchez Martínez, S., Díez Fernández, R., Martín Parra, L.M., Matas, J., Andonaegui, P., Fernández-Suárez, J., 2021. Geochemistry and Sm–Nd isotopic sources of Late Ediacaran siliciclastic series in the Ossa–Morena Complex: Iberian–Bohemian correlations. International Journal of Earth Sciences, 110(2), 467-485. DOI: https://doi.org/10.1007/s00531-020-01963-0

de la Rosa, J.D., Jenner, G.A., Castro, A., 2002. A study of inherited zircons in granitoid rocks from the South Portuguese and Ossa-Morena Zones, Iberian Massif: support for the exotic origin of the South Portuguese Zone. Tectonophysics, 352(1), 245-256. DOI: https://doi.org/https://doi.org/10.1016/S0040-1951(02)00199-3

Rosa, D.R.N., Finch, A.A., Andersen, T., Inverno, C.M.C., 2008. U-Pb geochronology of felsic volcanic rocks hosted in the Gafo Formation, South Portuguese Zone: the relationship with Iberian Pyrite Belt magmatism. Mineralogical Magazine, 72(5), 1103-1118. DOI: https://doi.org/10.1180/minmag.2008.072.5.1103

Rubio Pascual, F.J., Matas, J., Martín Parra, L.M., 2013. High-pressure metamorphism in the early Variscan subduction complex of the SW Iberian Massif. Tectonophysics, 592, 187-199. DOI: https://doi.org/10.1016/J.TECTO.2013.02.022

Sánchez-García, T., Chichorro, M., Solá, A.R., Álvaro, J.J., Díez-Montes, A., Bellido, F., Ribeiro, M.L., Quesada, C., Lopes, J.C., Dias da Silva, Í., González-Clavijo, E., Gómez Barreiro, J., López-Carmona, A., 2019. The Cambrian-Early Ordovician Rift Stage in the Gondwanan Units of the Iberian Massif, In: Quesada, C., Oliveira, J.T. (eds.). The Geology of Iberia: A Geodynamic Approach: The Variscan Cycle. Regional Geology Review, Springer Cham, 27-74. DOI: https://doi.org/10.1007/978-3-030-10519-8_2

Satkoski, A.M., Barr, S.M., Samson, S.D., 2010. Provenance of Late Neoproterozoic and Cambrian Sediments in Avalonia: Constraints from Detrital Zircon Ages and Sm-Nd Isotopic Compositions in Southern New Brunswick, Canada. The Journal of Geology, 118(2), 187-200. DOI: https://doi.org/10.1086/649818

Saylor, J.E. Sundell, K.E., 2016. Quantifying comparison of large detrital geochronology data sets. Geosphere, 12(1), 203-220. DOI: https://doi.org/10.1130/GES01237.1

Schenk, P.E., 1997. Sequence stratigraphy and proveance on Gondwana's margin: The Meguma Zone (Cambrian to Devonian) of Nova Scotia, Canada. Geological Society of America Bulletin, 109(4), 395-409. DOI: https://doi.org/10.1130/0016-7606(1997)109<0395:SSAPOG>2.3.CO;2

Schofield, D.I., Horstwood, M.S.A., Pitfield, P.E.J., Crowley, Q.G., Wilkinson, A.F., Sidaty, H.C.O., 2006. Timing and kinematics of Eburnean tectonics in the central Reguibat Shield, Mauritania. Journal of the Geological Society, 163(3), 549-560. DOI: https://doi.org/10.1144/0016-764905-097

Shellnutt, J.G., Owen, J.V., Yeh, M.-W., Dostal, J., Nguyen, D.T., 2019. Long-lived association between Avalonia and the Meguma terrane deduced from zircon geochronology of metasedimentary granulites. Scientific Reports, 9(1), 4065. DOI: https://doi.org/10.1038/s41598-019-40673-9

Simancas, J.F., 1983. Geología de la extremidad oriental de la Zona Sudportuguesa. Doctoral Thesis. Granada (España), Universidad de Granada, Unpublished, 487pp.

Simancas, J.F., Tahiri, A., Azor, A., Lodeiro, F.G., Martínez Poyatos, D.J., El Hadi, H., 2005. The tectonic frame of the Variscan–Alleghanian orogen in Southern Europe and Northern Africa. Tectonophysics, 398(3), 181-198. DOI: https://doi.org/https://doi.org/10.1016/j.tecto.2005.02.006

Simancas, J.F., 2019. Variscan Cycle. In: Quesada, C., Oliveira, J.T. (eds.). The Geology of Iberia: A Geodynamic Approach. Regional Geology Reviews, Springer Cham, 1-25. DOI: https://doi.org/10.1007/978-3-030-10519-8_1

van Staal, C.R., Whalen, J.B., Valverde-Vaquero, P., Zagorevski, A., Rogers, N., 2009. Pre-Carboniferous, episodic accretion-related, orogenesis along the Laurentian margin of the northern Appalachians. London, The Geological Society, Special Publication, 327, 271-316. DOI: https://doi.org/10.1144/SP327.13

van Staal, C.R., Barr, S.M., Waldron, J.W.F., Schofield, D.I., Zagorevski, A., White, C.E., 2021a. Provenance and Paleozoic tectonic evolution of Ganderia and its relationships with Avalonia and Megumia in the Appalachian-Caledonide orogen. Gondwana Research, 98, 212-243. DOI: https://doi.org/https://doi.org/10.1016/j.gr.2021.05.025

van Staal, C.R., Barr, S.M., McCausland, P.J.A., Thompson, M.D., White, C.E., 2021b. Tonian–Ediacaran tectonomagmatic evolution of West Avalonia and its Ediacaran–early Cambrian interactions with Ganderia: an example of complex terrane transfer due to arc–arc collision? London, The Geological Society, 503(1, Special Publications), 143-167. DOI: https://doi.org/10.1144/SP503-2020-23

Stern, R.J., Ali, K.A., Liégeois, J.P., Johnson, P.R., Kozdroj, W., Kattan, F.H., 2010. Distribution and significance of pre-Neoproterozoic zircons in juvenile Neoproterozoic igneous rocks of the Arabian-Nubian Shield. American Journal of Science, 310(9), 791-811. DOI: https://doi.org/10.2475/09.2010.02

Valenzuela, A., Donaire, T., Pin, C., Toscano, M., Hamilton, M.A., Pascual, E., 2011. Geochemistry and U–Pb dating of felsic volcanic rocks in the Riotinto–Nerva unit, Iberian Pyrite Belt, Spain: crustal thinning, progressive crustal melting and massive sulphide genesis. Journal of the Geological Society, 168(3), 717-732. DOI: https://doi.org/10.1144/0016-76492010-081

Vermeesch, P., 2018. IsoplotR: A free and open toolbox for geochronology. Geoscience Frontiers, 9(5), 1479-1493. DOI: https://doi.org/https://doi.org/10.1016/j.gsf.2018.04.001

Waldron, J.W.F., White, C.E., Barr, S.M., Simonetti, A., Heaman, L.M., 2009. Provenance of the Meguma terrane, Nova Scotia: Rifted margin of early Paleozoic Gondwana. Canadian Journal of Earth Sciences, 46(1), 1-8. DOI: https://doi.org/10.1139/E09-004

Waldron, J.W.F., Schofield, D.I., Dufrane, S.A., Floyd, J.D., Crowley, Q.G., Simonetti, A., Dokken, R.J., Pothier, H.D., 2014. Ganderia-Laurentia collision in the Caledonides of Great Britain and Ireland. Journal of the Geological Society, 171(4), 555-569. DOI: https://doi.org/10.1144/jgs2013-131

Warsame, H.S., McCausland, P.J.A., White, C.E., Barr, S.M., Dunning, G.R., Waldron, J.W.F., 2020. Meguma terrane orocline: U–Pb age and paleomagnetism of the Silurian Mavillette gabbro, Nova Scotia, Canada. Canadian Journal of Earth Sciences, 58(4), 315-331. DOI: https://doi.org/10.1139/cjes-2020-0089

White, C.E., Barr, S.M., Linnemann, U., 2018. U-Pb (zircon) ages and provenance of the White Rock Formation of the Rockville

Notch Group, Meguma terrane, Nova Scotia, Canada: evidence for the "Sardian gap" and West African origin. Canadian Journal of Earth Sciences, 55(6), 589-603. DOI: https://doi.org/10.1139/cjes-2017-0196

Willner, A.P., Bar, S.M., Gerdes, A., Massonne, H.J., White, C.E., 2013. Origin and evolution of Avalonia: Evidence from U-Pb and Lu-Hf isotopes in zircon from the Mira terrane, Canada, and the Stavelot-Venn Massif, Belgium. Journal of the Geological Society, 170(5), 769-784. DOI: https://doi.org/10.1144/jgs2012-152

Žák, J., Svojtka, M., Gerdjikov, I., Kounov, A., Vangelov, D.A., 2021. The Balkan terranes: a missing link between the eastern and western segments of the Avalonian–Cadomian orogenic belt? International Geology Review, 64(17), 2389-2415. DOI: https://doi.org/10.1080/00206814.2020.1861486

Zhang, W., Pease, V., Whitehouse, M.J., El-Sankary, M.M., Shalaby, M.H., 2019. Pre-Neoproterozoic basement evolution of southwestern Egypt. International Geology Review, 61(15), 1909-1926. DOI: https://doi.org/10.1080/00206814.2018.1552842

Zimmermann, U., Andersen, T., Madland, M.V., Larsen, I.S., 2015. The role of U-Pb ages of detrital zircons in sedimentology—An alarming case study for the impact of sampling for provenance interpretation. Sedimentary Geology, 320, 38-50. DOI: https://doi.org/https://doi.org/10.1016/j.sedgeo.2015.02.006

Manuscript received December 2021;
revision accepted September 2022;
published Online December 2022.

APPENDIX I

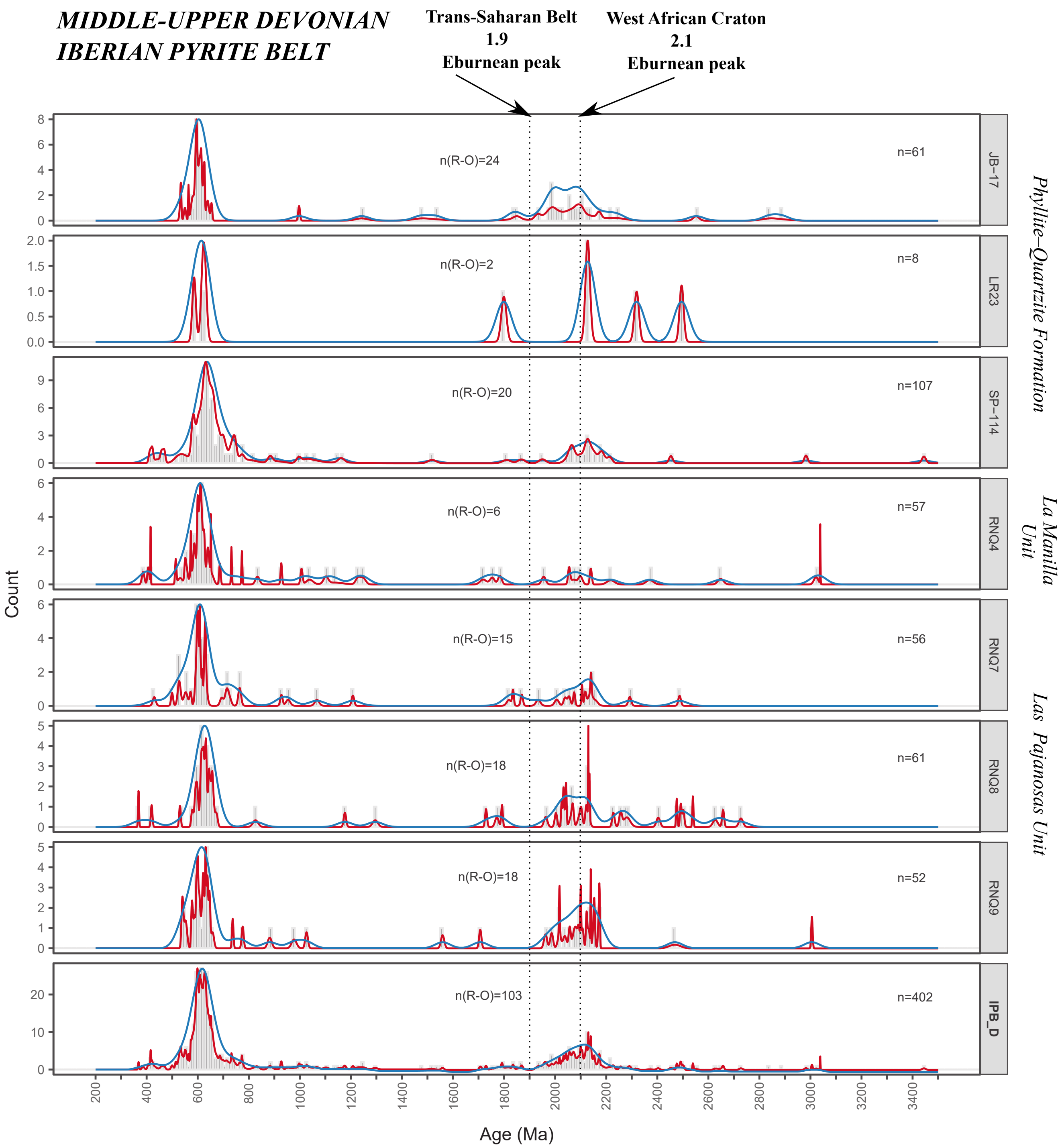

FIGURE I. Kernel density estimation and probability density plots for the individual samples (JB-17: Braid *et al.*, 2011; SP-114: Pereira *et al.*, 2012; LR23: Rosa *et al.*, 2008; RNQ4, RNQ7, RNQ8, RNQ9: Pérez-Cáceres *et al.*, 2017), and combined sample IPB_D (bottom image) of the Middle-Upper Devonian quartzites of the Iberian Pyrite Belt. n(R-O): number of Rhyacian-Orosirian analyses.

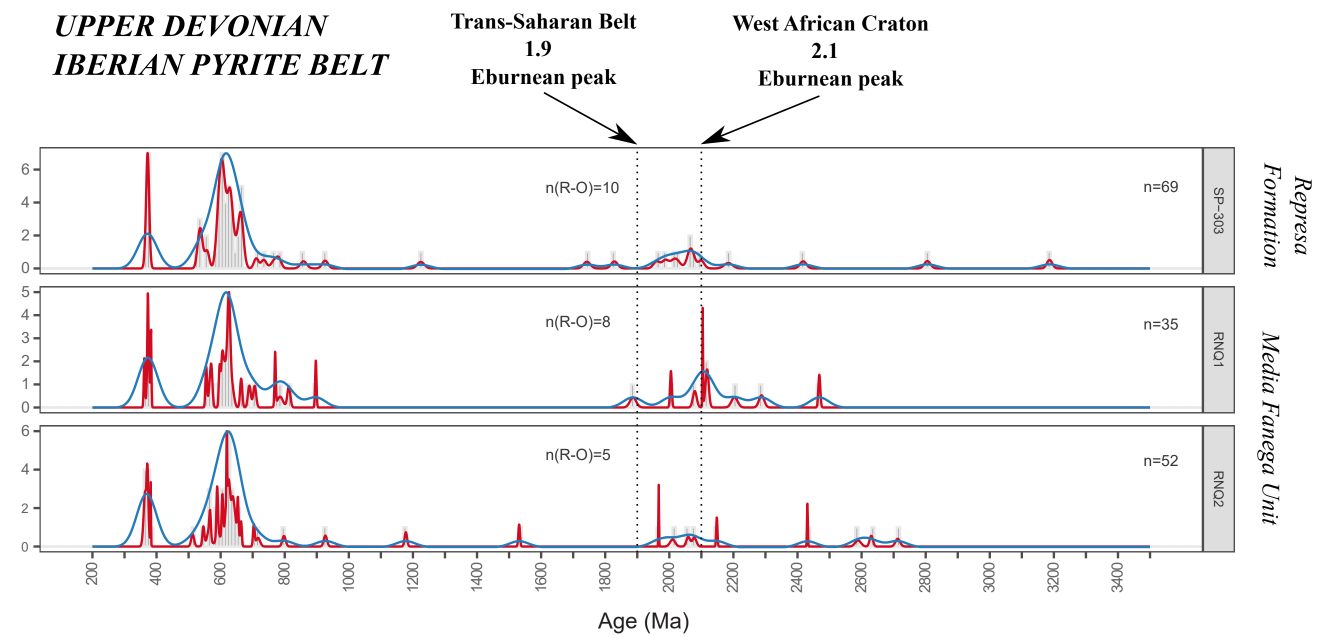

FIGURE II. Kernel density estimation and probability density plots for the individual samples (SP-303: Pereira *et al.*, 2017; RNQ1, RNQ2: Pérez-Cáceres *et al.*, 2017) of the Upper Devonian quartzwackes and greywackes of the Iberian Pyrite Belt. n(R-O): number of Rhyacian-Orosirian analyses.

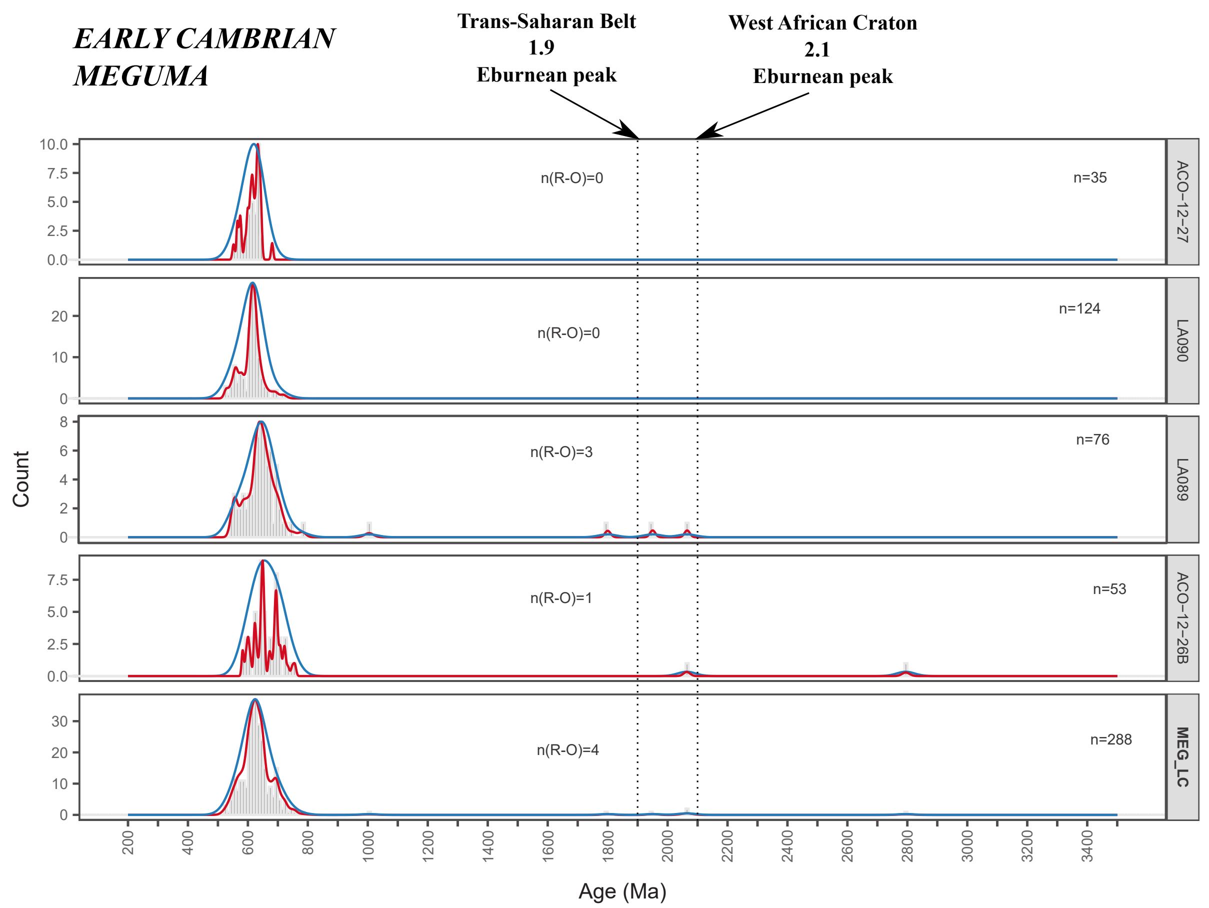

FIGURE III. Kernel density estimation and probability density plots for the individual samples (ACO-12-27, ACO-12-26B: Henderson *et al.*, 2016; LAO90, LA089: Waldron *et al.*, 2009), and combined sample MEG_LC (bottom image) of the lower Cambrian detrital rocks of the West Meguma terrane.

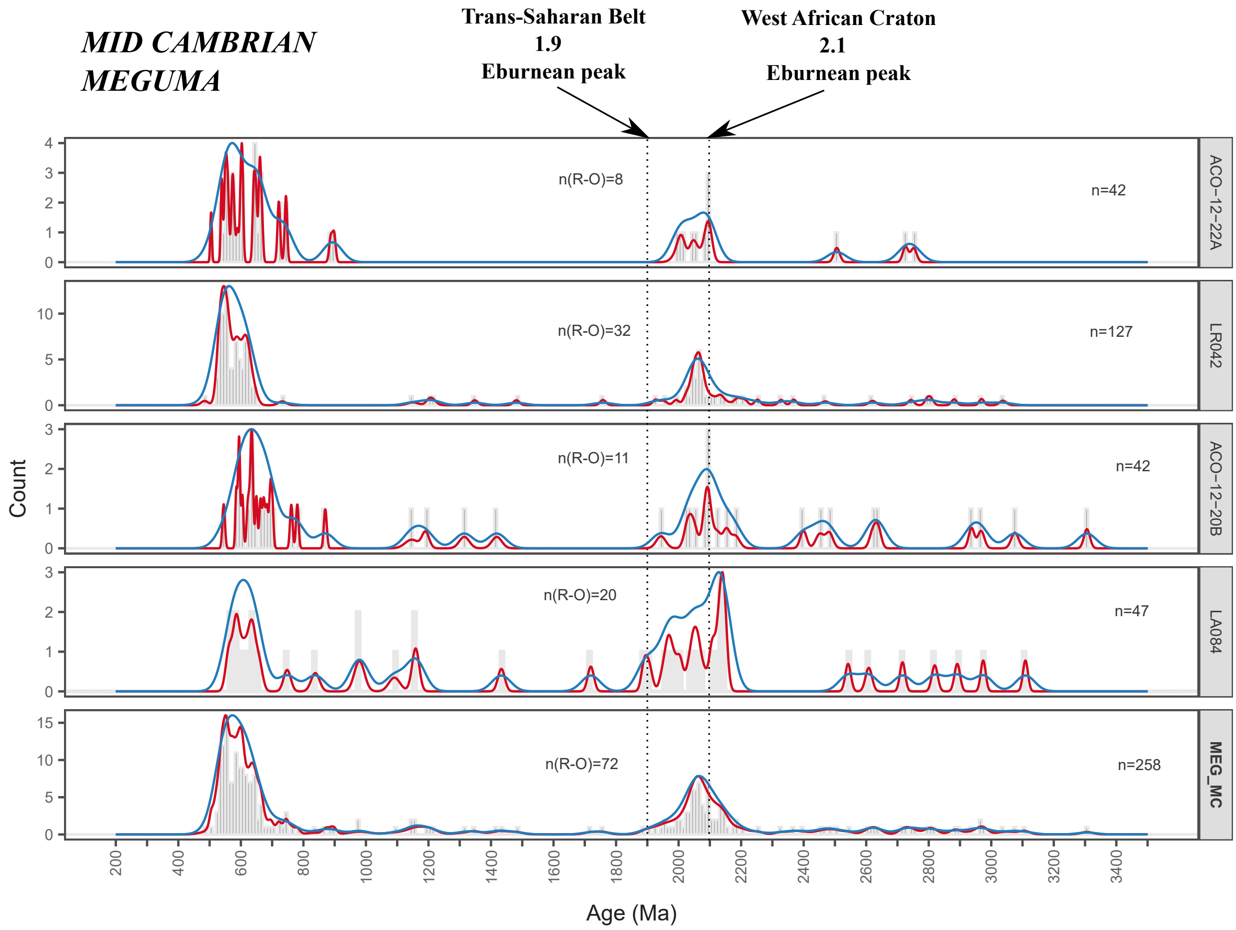

FIGURE IV. Kernel density estimation and probability density plots for the individual samples (ACO-12-22A, ACO-12-20B: Henderson *et al.*, 2016; LR042, LA084: Waldron *et al.*, 2009), and combined sample MEG_MC (bottom image) of the middle Cambrian detrital rocks of the West Meguma terrane.

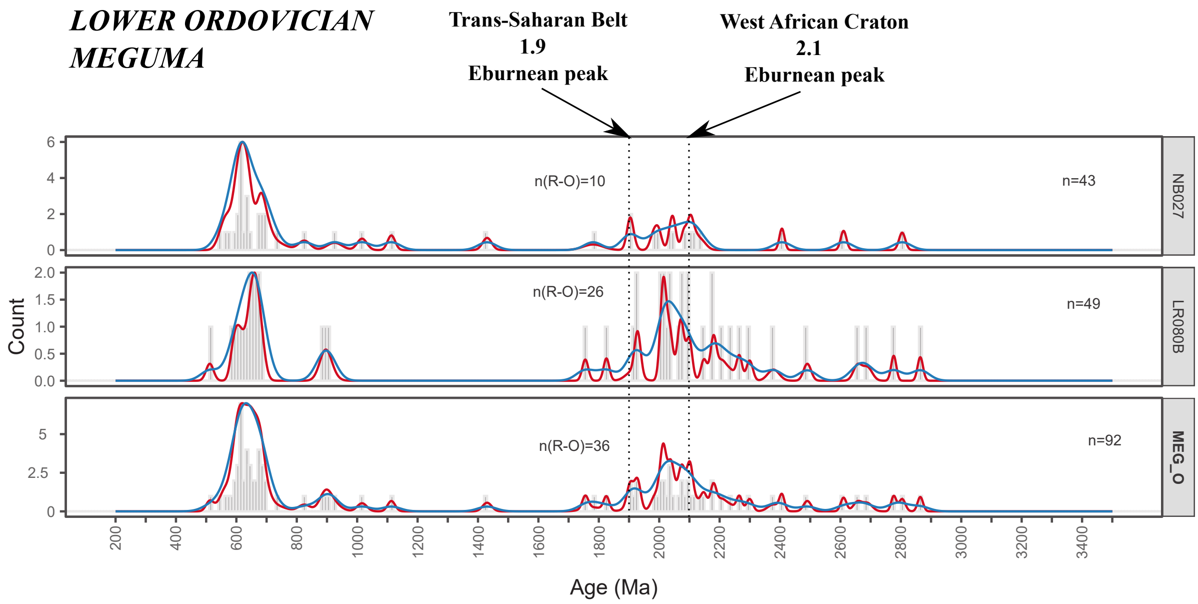

FIGURE V. Kernel density estimation and probability density plots for the individual samples (NB027, LR080B: Pothier *et al.*, 2015), and combined sample MEG_LO (bottom image) of the Lower Ordovician detrital rocks of the West Meguma terrane.

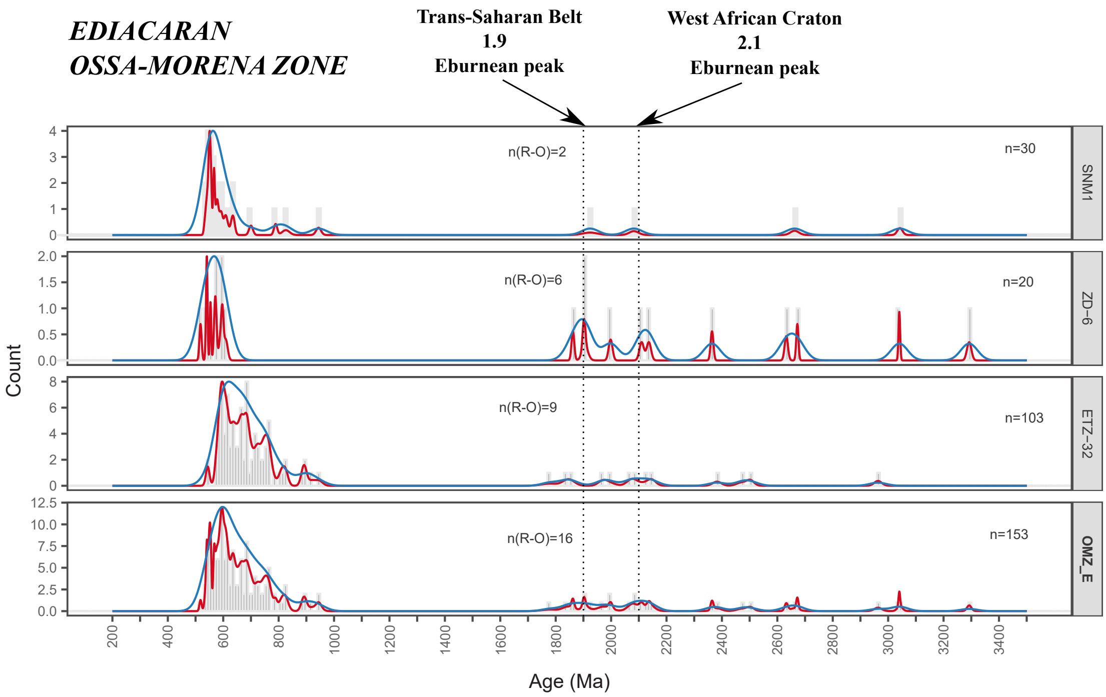

FIGURE VI. Kernel density estimation and probability density plots for the individual samples (SNM1: Linnemann *et al.*, 2008; ZD-6: Fernández-Suárez *et al.*, 2002; ETZ-32: Pereira *et al.*, 2012), and combined sample OMZ_E (bottom image) of the Ediacaran detrital rocks of the Ossa-Morena Zone.

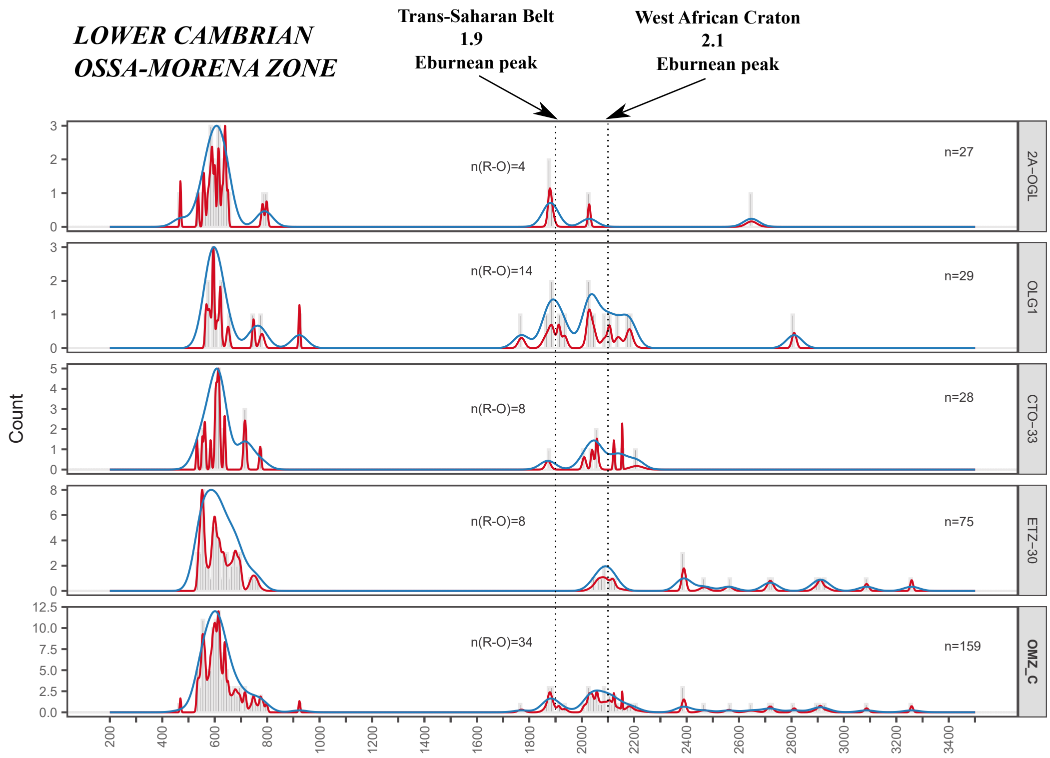

FIGURE VII. Kernel density estimation and probability density plots for the individual samples (2A-OGL, OLG: Linnemann *et al.*, 2008; CTO-33, ETZ-30: Pereira *et al.*, 2011), and combined sample OMZ_LC (bottom image) of the lower Cambrian detrital rocks of the Ossa-Morena Zone.

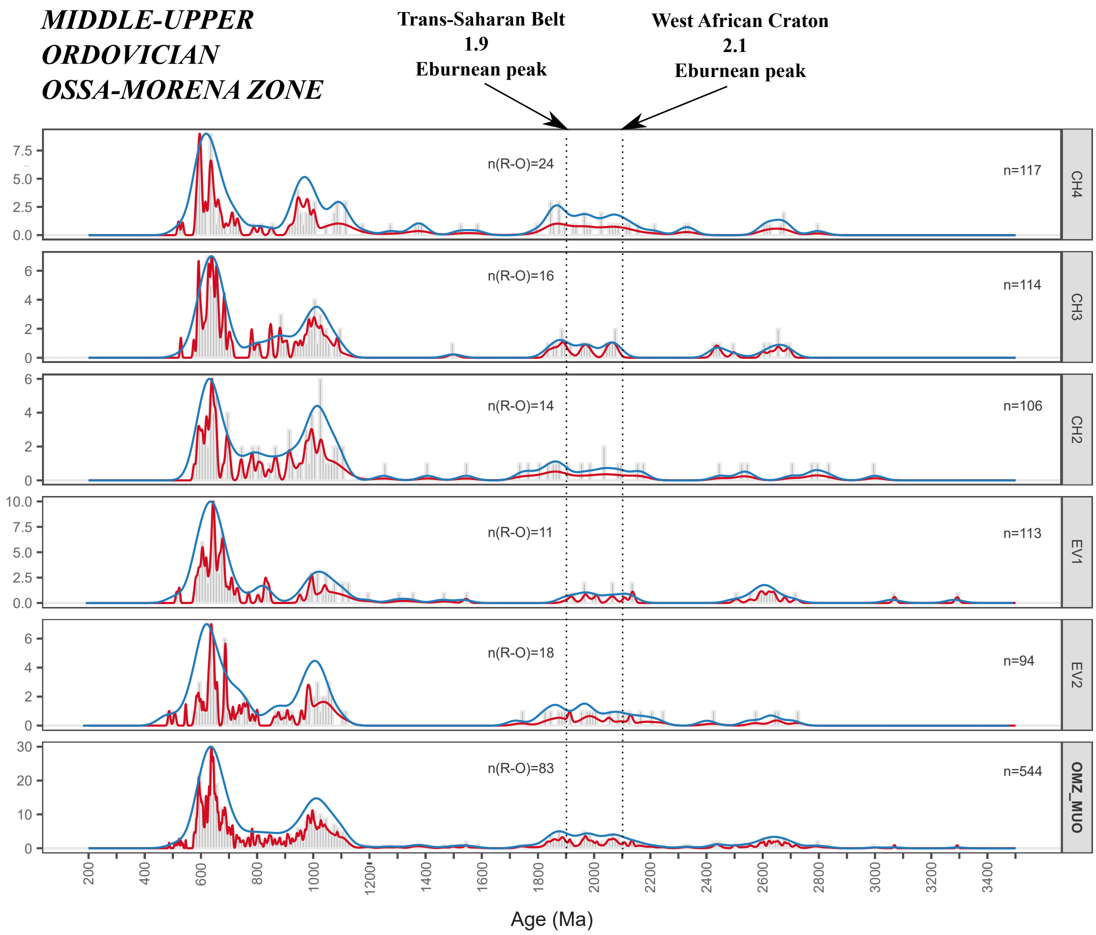

FIGURE VIII. Kernel density estimation and probability density plots for the individual samples (CH4, CH3, CH2, EV1, EV2: Azor *et al.*, 2021), and combined sample OMZ_MUO (bottom image) of the Middle and Upper Ordovician detrital rocks of the Ossa-Morena Zone.

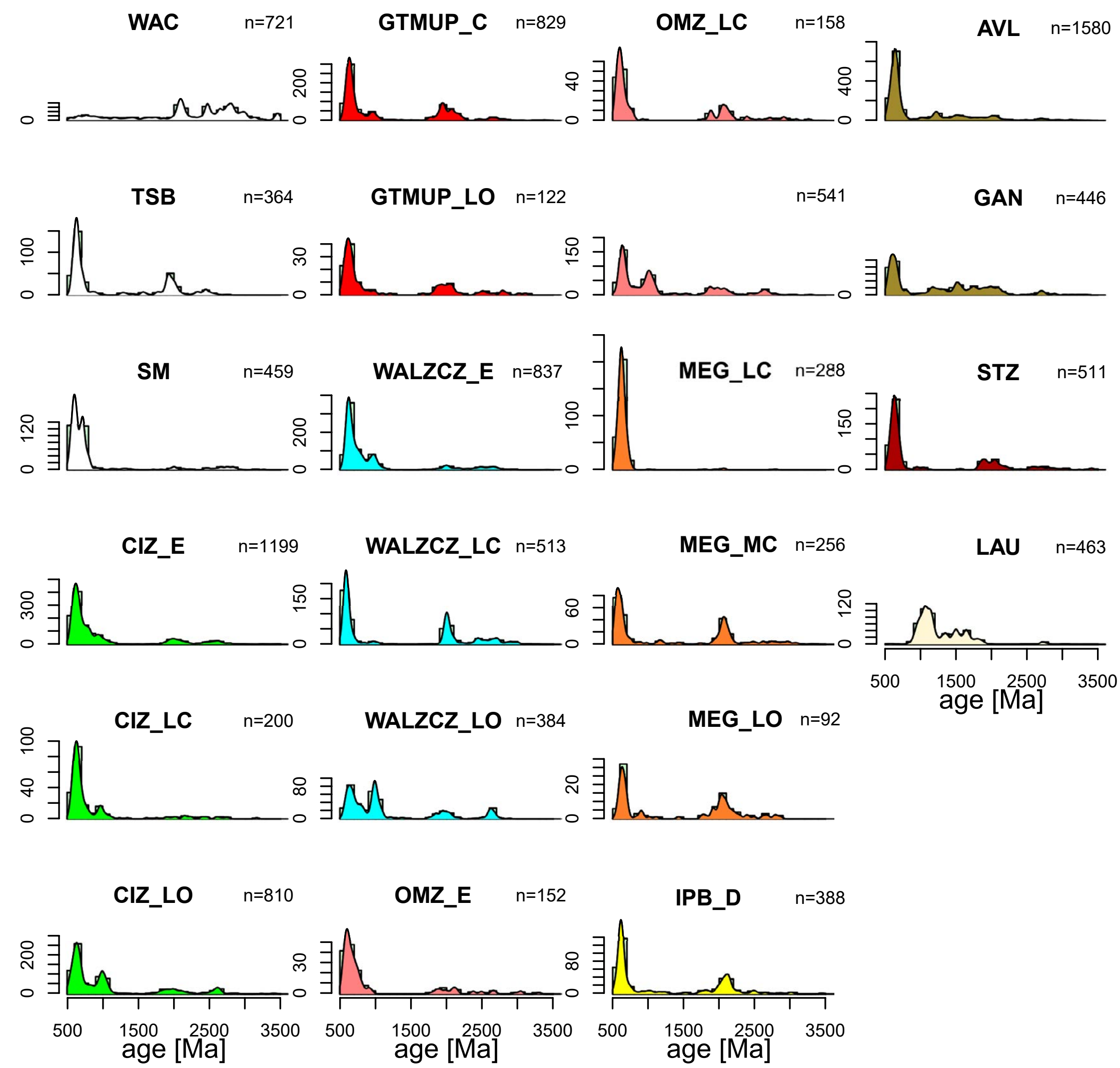

FIGURE IX. Normalized Kernel density estimations for analysis older than 520Ma.

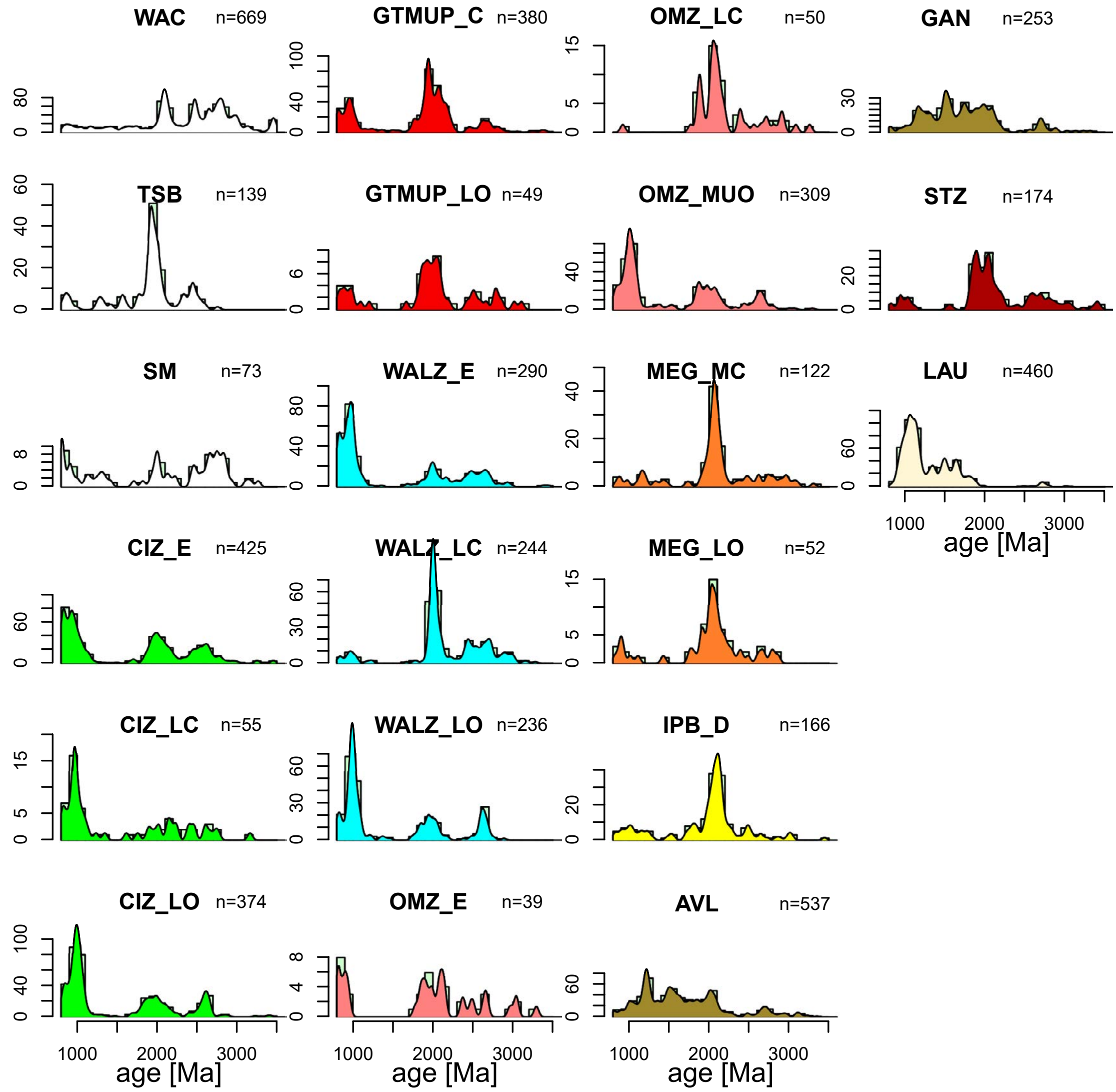

FIGURE X. Normalized Kernel density estimations for analysis older than 800Ma.

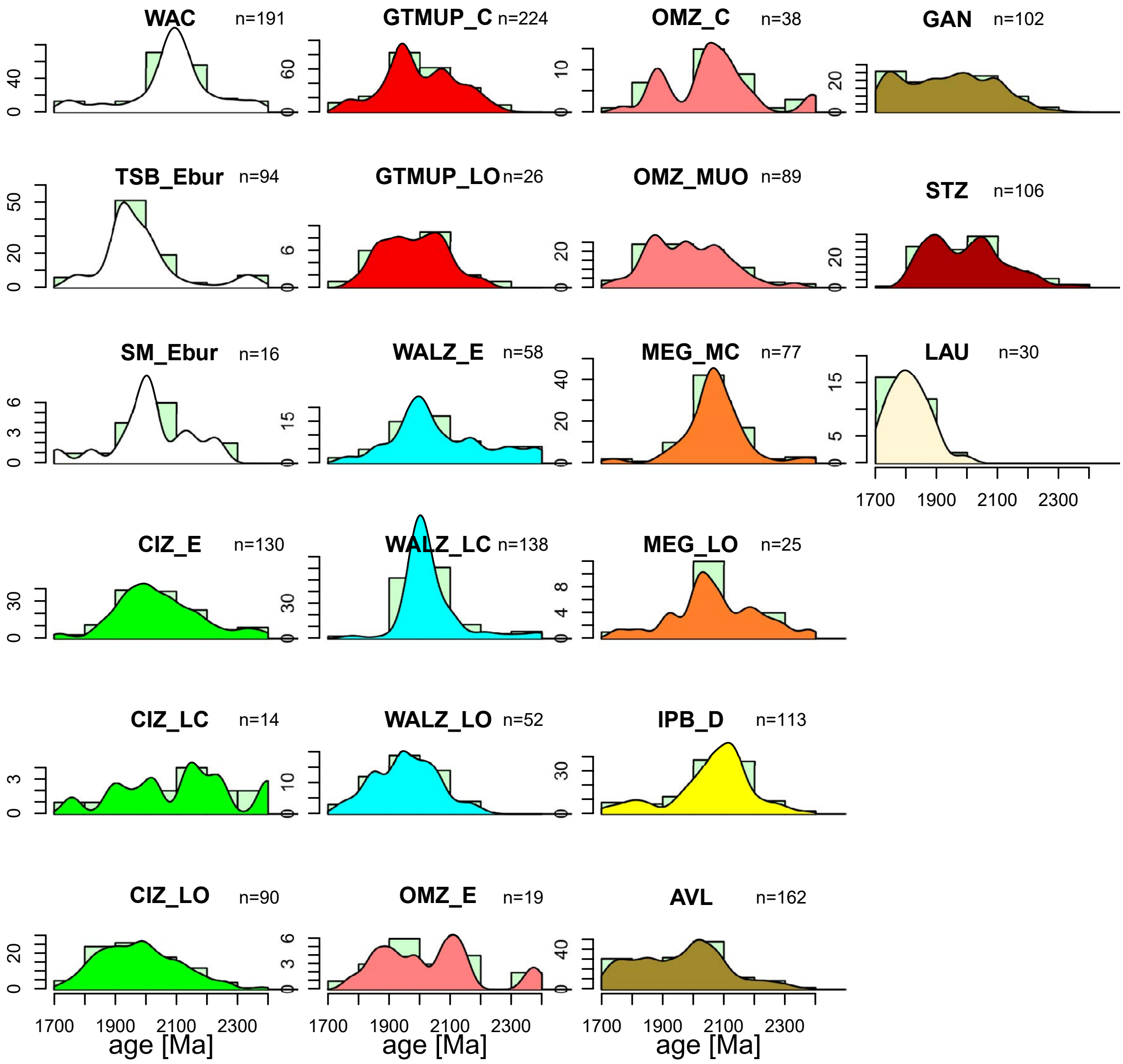

FIGURE XI. Normalized Kernel density estimations for analysis between 1700 and 2400Ma.